Title

Interpreting Pleistocene Predator-Prey Dynamics: Inference from Skeletal Pathology, Dental Growth and Stature

Permalink

https://escholarship.org/uc/item/3qm426gv

Author

Brown, Caitlin Anna-Corbett

Publication Date

2017

Peer reviewed|Thesis/dissertation

UNIVERSITY OF CALIFORNIA

Los Angeles

Interpreting Pleistocene Predator-Prey Dynamics: Inference from Skeletal Pathology, Dental

Growth and Stature

A dissertation submitted in partial satisfaction of the requirements for the

degree Doctor of Philosophy in Biology

by

Caitlin Anna-Corbett Brown

2017

ABSTRACT OF THE DISSERTATION

Interpreting Pleistocene Predator-Prey Dynamics: Inference from Skeletal Pathology, Dental

Growth and Stature

by

Caitlin Anna-Corbett Brown

Doctor of Philosophy in Biology

University of California, Los Angeles, 2017

Professor Blaire Van Valkenburgh, Chair

Mammalian teeth and bone contain a record of an animal's health and environment over daily,

weekly, and yearly time scales. These tissues have long been used to assess the health and

environmental conditions particular to individuals, but they may also preserve characteristics of

entire populations, in this case relative population size and behavior. In this dissertation, we draw

new inferences from skeletal and dental characters to demonstrate that they preserve 1) unique

signals of predatory behavior and 2) relative changes in ungulate population size. Chapter 1

assesses the potential of skeletal pathology to preserve a signal of behavior in extinct species,

specifically the hunting modes of two Pleistocene predators reconstructed as ambush and pursuit

predators, respectively. To answer this question we analyzed injury rates across thousands of

pathological elements and performed quantitative analysis of injury locations, the first such

application of spatial analyses. In chapter 2, we documented a correlation between population size, nutritional status and dental/osteological features in extant moose (*Alces alces*) using mandibles collected over the past five decades from Isle Royale, MI. This is the first attempt to use patterns of dental growth and wear in past or present populations to infer food-limitation and relative density. In chapter 3 we examined incremental growth rates of dentin, the tooth tissue surrounding the pulp cavity, allowing a first look at the responses of tooth enamel, dentin and bone growth to episodes of stress in a wild population. Through this work we developed methods of characterizing past ecosystems to benefit studies that seek to restore national parks to their pre-anthropogenic state or contribute to the long-standing paleontological debate regarding the Pleistocene mammal extinctions. As a result of our efforts, we have a robust set of both macroscopic and microscopic indicators of predatory behavior (Chapter 1) and nutritional stress (Chapter 2-3) that can be applied to extinct and extant carnivoran and ungulate and populations.

The dissertation of Caitlin is approved.

David K. Jacobs

Mike Alfaro

Shane White

Blaire Van Valkenburgh, Committee Chair

University of California, Los Angeles

2017

DEDICATION

To family and friends. You have given me all the support I could ask for, through listening ears, airport rides, equipment loans, couches to crash on, coffee and pastries, moral support, morale support, wardrobe assistance and sage advice. You have unlocked so many doors for me, figuratively and literally. Dedicating this work to you is the least I can do to thank you.

TABLE OF CONTENTS

LIST OF TABLES

ACKNOWLEDGEMENTS

I appreciate **Dr. Blaire Van Valkenburgh** for being the ideal mentor and role model. I am so thankful for your guidance in conducting research, navigating conferences and engaging audiences. When missed flights, lost catalogues or application errors seemed to have cost me everything, you were there with encouragements to persevere and try another approach. Most of all, I am thankful I had the opportunity learn how to instruct from you. The evolution of vertebrates is a complex story and no one tells it like you do, let alone in 10 weeks. I will always try to be as engaging, witty and vivacious as you are in the classroom.

Beth Rinaldi, I can't thank you enough for adopting me as a graduate student and a family member. As a mentor, I admire your meticulous and objective approach to gathering data, and also your open-mindedness. How many PI's would have helped construct the Home Depot lab? As a friend, I cannot thank you enough for taking time out of your action-packed days to impart some well-thought out wisdom. I cannot articulate how meaningful it was to see a mother balance instruction, science and family to guide so well and be successful in every one of them.

To the Van Valkyries and Van Valkenburgers, past and present: **Deborah Bird**, thank you for always being honest, in and out of academics. I admire your desire to wholly understand every idea you engage and I will be asking myself "Would Bird have any questions?" about every talk I write in the future. Thank you for making me a better communicator.

Benison Pang, it is so admirable that you report everything from basic descriptive studies to transformative evolutionary medicine with the same clear-eyed and direct manner. Reporting the news without a great story is much harder than crafting a narrative, but you always make it look easy. I don't know what you'll do in the future because you are more about the journey than the destination, and that's why I'm so glad I'm taking the journey with you.

Mairin Balisi, as a coworker I admire your willingness to consider alternative viewpoints and treat everyone's contributions with respect. As a scientist, I appreciate your methodical approach to every question. To me you embody the best, fairest and most honest practices in academia and I think you will be a boon to paleontology on so many levels.

Abigail Curtis, you taught me to navigate graduate school and how to be thick skinned enough to progress and improve. I'm able to discern the details worth sweating because of you.

Tony Friscia, you have the greatest laugh at UCLA. You enrich every discussion with wit, wide-ranging knowledge and levity in a way no one else does. Presenting our poster, I was struck by how many people came over, excited to see you and the universally positive things I heard about you. Professionally, you have shown me how to balance work, enjoy life and serve to our field. You are a great role model on many levels.

To my doctoral committee: **David Jacobs**, **Michael Alfaro**, and **Shane White**, and **Tim Cole**, **Greg Erickson**, **Gary Schwartz**, **Tim Cobb, Alan Garfield, Chris Griffis, Rolf Peterson** and **John Vucetich**, thank you for your advice and support.

Jocelyn Yamadera, you merit a special mention for being zen and understanding of me at my most forgetful and worst. I have learned to be mindful of my administrative support through your persistent patience and will never forget your offer generosity when I was in dire financial straits.

To **my parents**, I owe you an academic debt for making me work in your hardware store all those years. I literally could not have completed chapter 3 without being comfortable with power tools, or getting your advice on which hole saws I should use on enamel vs bone, or being shown how to cut through glass microscope slides without ruining the irrepoacable teeth glued to them. Not many people get to call their parents for help with their PhD, I imagine. Similarly, I

thank **Uncle Ron** for teaching me to use the band saw, drill press and belt sander, essential tools for chapters 2 and 3. Most of all, you all taught me to believe I can do anything- you can learn any skill, but confidence is much harder to impart.

VITA

EDUCATION

Doctor of Philosophy in Biology at the University of California, Los Angeles, September 2010-

Present. Expected 2017. Dissertation Title: Interpreting Pleistocene Predator-Prey Dynamics:

Inference from Skeletal Pathology, Dental Growth and Stature

Bachelor of Science at the University of Notre Dame, 2010.

PUBLICATIONS

Brown C., Curd M., Friscia A. An Actualistic Experiment to Determine Skeletonization and

Disarticulation in the La Brea Tar Seeps. *Palaios.* 32.3 (2017): 119-124.

Brown C., Balisi M., Shaw C.A., Van Valkenburgh B. Skeletal Trauma Reflects Hunting

Behavior in the Extinct La Brea Sabertooth Cat and Dire Wolf. *Nature Ecology and Evolution*. 1

(2017): 0131.

PRESENTATIONS

Jan. 2016 Society for Integrative and Comparative Biology Annual Meeting. Poster Presentation:

"Skeletal Injury Distribution Reflects Hunting Behavior in Extinct Predators: a Novel

Application of GIS Technology"

Fall 2015 Society of Vertebrate Paleontology 75th Annual Meeting. Oral Presentation Title: "Macroscopic Enamel Indicators of Population-Wide Food Stress in Modern, Pleistocene, and Holocene Ungulates"

Fall 2014 Society of Vertebrate Paleontology 74th Annual Meeting. Poster Presentation Titles: "Dental Development Preserves Population Fluctuations in Wild Ungulates: The Present is the Key to the Past"

"An Actualistic Experiment to Examine Skeletonization and Disarticulation in the La Brea Tar Seeps".

Summer 2014. 1st Congress of the International Association for Paleodontology. Poster Presentation Title: " Dental Development Preserves Population Fluctuations in Wild Ungulates: The Present is the Key to the Past ".

Fall 2013 Society of Vertebrate Paleontology 73rd Annual Meeting. Poster Presentation Title: "What Can Paleopathology Tell Us About Hunting Modes?".

APPOINTMENTS

Lecturer, General Education Cluster, University of California, Los Angeles. 2015-2016.

Teaching Assistant, Department of Ecology and Evolutionary Biology, University of California, Los Angeles. 2011-2016.

CHAPTER 1

Skeletal Trauma Reflects Hunting Behavior In Extinct Sabertooth Cats And Dire Wolves

INTRODUCTION

The frequency and anatomical distribution of traumatic, chronic, and degenerative skeletal lesions record hazards encountered over a lifetime (1-5). For mammalian predators, the most common hazards pertain to hunting prey and aggression against other carnivores, which may leave signature distributions of injury across the skeleton. In particular, large carnivorans (>21kg) are likely more prone to hunting injury than smaller species because they are obligated to take prey that is similar in size to themselves or larger (6, 7). Among large carnivores, species that hunt their prey from ambush as opposed to pursuit might be expected to differ in the distribution of traumatic and chronic injuries. Spatial analysis of these pathologies should then reveal patterns of injury indicative of hunting behavior and thus can be used to infer hunting modes in species with no living analog. We examined pathologies from two co-occurring extinct predator species exceptionally well represented in the late Pleistocene fossil record: the dire wolf, *Canis dirus*, and the sabertooth cat, *Smilodon fatalis*. Here, we calculate both the absolute and relative frequency of trauma across the skeleton of both *C. dirus* and *S. fatalis.* By doing so, we are able to confirm that the skeletons of sabertooth cats suffered many more traumatic events than those of dire wolves, and that differences in distribution of the pathologies reflect their distinct hunting styles.

The Rancho La Brea asphalt seeps in Los Angeles, California, preserve an incomparable record of late Pleistocene life, ranging from arthropods to mammoths. The sticky asphalt seeps,

or "tar pits" as they are commonly known, acted as traps for unwary herbivores, such as bison, that then lured multiple carnivores, such as dire wolves, to their death. There are approximately nine times as many large carnivores as herbivores preserved in the Rancho La Brea collections (8) and the sample is dominated by dire wolves and *Smilodon*. There are estimated to be over five thousand well-preserved partial or full skeletons of these two species, a number that far exceeds the known sample for any extant large carnivore species. Consequently, it is possible to document the frequency and distribution of rare events, such as calcifying hematomas or healed fractures, in these two extinct predators.

We documented and analyzed skeletal elements that had been previously diagnosed as pathologic in *S. fatalis* and *C. dirus* that co-occurred over a 1000-year time span. All the bones are from a single deposit at Rancho La Brea, Pit 61/67, and were preserved in the asphalt approximately 11,500 years ago (12,200 +/- 200 to 11,130 +/- 275 ybp) (9). Pit 61/67 contained a minimum of 342 *S. fatalis* and 371 *C. dirus* represented by over 35,000 bones, nearly 2000 of which preserve one or more pathologies. To better visualize the data, we used Geographic Information Systems (GIS) software to map the density and distribution of pathologies. Our approach was inspired by previous studies that used spatial analysis to analyze anatomical samples, such as for mapping the distribution of skeletal elements across excavations (10,11), estimating the minimum number of individuals in a fossil assemblage (12), analyzing bone modifications across fossil and modern assemblages (13-15), and mapping pathological lesions in soft tissue (16).

Given the probable contrast in hunting style between sabertooth cats and dire wolves, we expected them to differ significantly in the distribution of healed fractures and other musculoskeletal trauma. Like extant gray wolves, dire wolves were cursorial pursuit predators

that apprehended and killed prey with their jaws alone (17,18). By contrast, *Smilodon,* a species without close modern analogs, is believed to have ambushed large prey, using powerful back and forelimb muscles to pull down and position prey for one or more killing bites (19-21). Consequently, injuries in *Smilodon* might be concentrated in the shoulder, anterior ribcage, and spine, whereas those of dire wolves might be more evenly distributed across all four limbs. In addition, head injuries might be more common in the dire wolves due to the risks of being kicked while biting the hindquarters during a chase (22, 23). Other than studies of dental fracture frequency (e.g. 24,25), injured bacula (26), isolated case reports (e.g. 27), and a doctoral dissertation (28), there has been little published work on the frequency of dire wolf paleopathologies. Previous studies of skeletal paleopathologies in the two species at Rancho La Brea found a greater number of pathological bones in *Smilodon* than *C. dirus* across all pits (5000 vs. 3200) (29), despite the fact that dire wolves are more common at Rancho La Brea. In addition, these authors reported numerous examples of injuries in *Smilodon* caused by excessive muscle strain (e.g., Fig. 1), as well as compression injuries to the ribcage and vertebrae that appear to be the result of forceful impact with prey (29-31). To better quantify the relative frequency of injury in these two species, our study examined both pathological and non-pathological elements, a task that required counting a large number (n > 35,000) of non-pathological specimens. These challenges may have limited previous studies of paleopathologies at Rancho La Brea, but now are manageable given advances in computerization and database software.

METHODS

Materials

Nearly 10,000 pathological bones of Pleistocene vertebrates from the Rancho La Brea asphalt seeps were previously diagnosed and set aside as a special collection by Christopher A. Shaw and Fred P. Heald, M.D. (30, 31). Of these, 1946 elements belong to either the dire wolves or sabertooth cats entrapped in Pit 61/67, and all but 92 of these elements represent adults. All pathological and non-pathological bones are housed at the La Brea Tar Pits and Museum in Los Angeles. Heald and Shaw (30) categorized pathologies based on their most probable etiology: dental pathologies, wounds, traumatic injuries, chronic re-injuries, and developmental anomalies. Traumatic injuries include various healed fractures and degenerative osteoarthritis, while chronic re-injuries refer to bony outgrowths at muscle attachment sites that reflect extreme muscle strain (Fig. 1.1). For this study, pathologies were condensed into three broad categories: traumatic injury (traumatic injury and chronic muscle, ligament and tendon re-injuries), infected wounds (e.g. bites), and other pathologies (e.g. developmental or unknown cause). Dental injuries were excluded. Each bone or partial bone in the pathological collection of *S. fatalis* and *C. dirus* from Pit 61/67 was examined by CB and MB. The diagnosis made by Shaw and Heald was recorded and the location of the pathology was noted on a diagram of the element or with a digital image.

Because we wished to compare the overall frequency of pathology in the two species, we counted the total number of non-pathological as well as pathological elements from Pit 61/67. Due to a low recovery of elements and/or a lack of identified non-pathological elements, total counts could not be obtained for the ribs of *Smilodon* as well as the sternebrae, terminal caudal vertebrae, and bones of the manus and pes for both *Smilodon* and *C. dirus*. While all *C. dirus* lumbar vertebrae were identified by position (e.g., L1, L2, L3), only 70% of *Smilodon* lumbar vertebrae were similarly identified. To estimate the total number of non-pathological lumbars present for *Smilodon*, we used the known proportion of pathological to non-pathological

elements in the sorted portion of the specimens. In doing so, we assumed that the composition of the sorted lumbars represented the whole.

Minimum Number of Individuals

Individual skeletons are almost always disarticulated and partially represented at Rancho La Brea, making it difficult to be sure of the number of individuals preserved. Following White (50), the minimum number of individuals was estimated as equivalent to the frequency of the most common identifiable element (1st cervical vertebra for dire wolf, 4th or 13 thoracic vertebra for *Smilodon*) of each species in the assemblage (Table 1.1*)*. Skeletal part representation was determined by generating MNI counts for each species. The count of a particular skeletal element or portion of an element was tallied per side and the most numerous count was used. This produced a conservative estimate of individual numbers.

Observed and Expected Frequency of Trauma

We analyzed injury frequency on a per bone basis by calculating the proportion of pathological to non-pathological bones for each element (e.g. humerus, scapula). This provided an estimate of the probability that a particular element will exhibit a pathology, and allowed us to compare injury frequencies for each bone between the two species. To compare overall rates of trauma across the entire skeleton between the two species, it was essential to take into account possible taphonomic bias in the frequency of preserved individual elements. For example, if *Smilodon* scapulae tend to be better represented than those of *C. dirus*, and if scapulae have a high rate of trauma, then the overall frequency of pathology would be inflated in *Smilodon* relative to *C. dirus*. To deal with this potential bias, we calculated an expected estimate of the

number of elements with trauma based on their relative frequency within the pit. For the

expected values, we calculated the frequency at which all elements would be injured if injuries

were evenly distributed, then multiplied the total number of each element in the sample by that

frequency to get an expected count. We compared the observed versus the expected number to

determine if the bone was injured at a higher rate than expected (Fig. 1.2, Table 1.2). We also

analyzed trauma frequency on a per bone basis by calculating the proportion of all bones with

trauma for each element (e.g. humerus, scapula). These data were used to compare trauma

frequencies for each bone between the two species (Table 1.3). Statistical significance of all

differences in frequency was tested by a G test of independence using the analysis software R

(www.R-project.org) and the package DescTools. The G test of independence is a proportions

test similar to chi-squared test; a description of the test can be found in the Handbook of

Biological Statistics (3rd ed.). Sparky House Publishing, Baltimore, Maryland. Pp 68-76.

Spatial Analyses

In addition, we tested the utility of geographic information systems (GIS)

technology in visualization and analysis of pathology locations across a complete skeletal map.

Pathologies were digitized as polygonal features on a single skeleton "base map" using ArcMap

10.2.2 ArcGIS® software by ESRI (Fig. 1.3). Individual pathologies diagnosed as trauma were

translated into vector polygons using hand-drawn representations of the skeletal pathologies

(75%) or photographs (25%). All pathologies were mapped to the left side in lateral view for

clarity, compressing all pathologies into a two-dimensional plane (Figure 1.4). Original

orientation (e.g. medial, cranial) was stored as an attribute of the polygon allowing orientations

to be filtered if desired. Polygons were not used for spatial analysis but were converted into

centroids. Thus each pathology was represented by a single centroid or point on the skeletal maps.

Polygon centroids were calculated and used for all spatial analyses. All pathologies were mapped to the left side in lateral view for clarity, compressing all pathologies into a two-dimensional plane. Injuries to the sternebrae were mapped as evenly distributed because the exact identity (e.g. first, second, etc.) of the pathological sternebrae cannot be determined. Because phalanges were not identified as belonging to either manus or pes in *C. dirus*. We mapped all phalanges to both manus and pes, artificially doubling the number of injuries to the phalanges but preserving the spatial relationships.   Data analysis was conducted using the Spatial Analyst extension using methods first developed by Parkinson and colleagues (13-15) for analysis of the distribution of carnivore tooth marks on bones. The resulting heat maps were further analyzed using Optimized Hotspot Analysis. The pathology database can be filtered by attributes such as pathology type, afflicted bone, and location; only the most common types of injuries, those we classified as traumatic, are analyzed here. The majority of injuries common to *Canis dirus* and *Smilodon fatalis* were chronic injuries (56.4-85.1%), followed by fractures (10-14%) and wounds (<5%).

For our analyses, we merged putative chronic, fracture, and osteoarthritic injuries into a single category, trauma. Chronic injuries consistent with hunting mode dominate the pathology collection in both species, and thus the density maps likely capture pathologies predominately resulting from prey capture. Wound distribution is broadly similar to that of traumatic injury (Fig. 1.4); thus, the injuries classified as traumatic may include some injuries caused by conflict with other carnivorans. However, we deduce that the preponderance of the

traumatic pathologies was incurred by hunting because of their anatomical position and the hunting mode of each predator.

Optimized Hot Spot Analysis (OHSA) determines an appropriate scale of analysis and uses the scaled cells to detect statistically significant areas of density and voids in pathology centroids across the entire skeleton (51). This process objectively distinguishes hotspots, or cells with injury density significantly greater than the mean, across the skeleton. Following the method of Parkinson and colleagues (13,14) the Average Nearest Neighbor Distance (ANND) tool was used to test for significant clustering of centroids within a defined region (cranium, each vertebral region, forelimb, manus, ribcage, pelvis + sacrum, hindlimb, pes). Pathology distribution is considered clustered if the average distance between centroids is less than expected for a hypothetical random distribution over the area being analyzed (52). The kernel density function was used to produce heat maps that illustrate areas of frequent injury (Fig. 1.5). Sternebrae, manus, and pes for both species and the ribs for *Smilodon* only were included in the spatial analysis but were excluded from the statistical analyses above.

Average nearest neighbor distance (ANND) was used to test for significant clustering of traumatic+chronic centroids within a defined region. We defined 11 regions: cranium, each vertebral region, forelimb, manus, ribcage, pelvis+sacrum, hindlimb, pes. Pathology distribution is considered clustered if the average distance between centroids is less than expected for a hypothetical random distribution over the area being analyzed. *Smilodon* cranial and all caudal injuries were not analyzed due to insufficient pathology counts in those regions.

RESULTS

Minimum Number of Individuals.

Based on the most common axial element, we estimated that a minimum of 342 *S. fatalis* and 371 *C.* were preserved in Pit 61/67 (Table 1.1). Thus, the two are nearly equally represented in Pit 61/67, and differences in absolute frequency of skeletal pathologies are not due to a preponderance of one species in the collection.

Overall Frequency of Traumatic Injury.

We first quantified the frequency of combined traumatic and chronic injuries in each species (hereafter simply referred to as "trauma"). The total number of pathological elements in *Smilodon* is greater than in the dire wolf (781 vs. 554, Table 1.1) and this results in a traumatic pathology frequency for the sabertooth cat that is significantly higher (4.3% in *Smilodon*, 2.8% in *C. dirus*, G=59.389, p<.001). Evidence of wounds was much less frequent in both species (<5%), and pathologies of unknown cause or due to developmental defects make up the balance (11.2%-39.3%). In this study, we consider only trauma, the injuries likely to result from hunting which include healed fractures and evidence of severe or chronic muscle strain, as well as osteoarthritis.

Distribution of Traumatic Injury Based on Observed Injury Frequency.

Within each species, the frequency of trauma across skeletal elements is significantly different from uniform (Fig. 1.2; *Smilodon* G=941.75, p<2.2 e-16; *C. dirus*, G=307.17, p<2.2 e-16; Table 1.2). As predicted, *Smilodon* injuries were prevalent in the spinal column, accounting for 56% of all pathologies, but contrary to expectation, they were uncommon on the shoulder, sternum or ribs (Fig. 1.5a). The most frequently injured elements belonged to the lumbar region of the spine and thoracic vertebrae medial to the scapula. The frequency of sacral injuries was

9

low, but this may be an underestimate because the first three sacral vertebrae were frequently disarticulated and poorly preserved. Traumatic injuries in *C. dirus* were more evenly distributed across the skeleton (Fig. 1.5b). As predicted, the limbs of *C. dirus* were injured more frequently than those of *Smilodon* despite overall lower rates of injury. Limb injuries represent 64.6% of all dire wolf traumatic injuries and only 22.7% in *Smilodon.*

Observed vs Expected Frequency of Traumatic Injury.

When bias in the numbers of preserved elements is accounted for, *Smilodon* injuries are significantly more frequent than expected for the scapula even though the overall frequency of injury is low. Frequencies were also higher than expected for *Smilodon's* thoracolumbar spine (eleventh thoracic vertebra [T11] through seventh lumbar vertebra [L7]) but not the distal limbs (Fig. 1.5a). Evidence of trauma to the cranium, first cervical vertebra (C1), and humerus was significantly less than expected given their numbers in the sample. We expected the dire wolf cranium to be injured frequently, and while it was more often injured than in *Smilodon*, the injuries did not exceed the expected frequency. However, the first three cervical vertebrae (C1-C3) of the dire wolf had higher than expected frequencies, as did the sacrum, innominate, and most limb bones (femur, tibia, fibula, radius, ulna) except the scapula.

Spatial Analyses.

The heat maps (Figs. 1.5a, 1.5c, 1.6) of trauma frequency across the two skeletons support the above results and also reveal more precisely the locations of the trauma. In *Smilodon*, the thoracic vertebrae at the shoulder girdle and thoracolumbar junction show concentrations of trauma in these locations. Pathology density increases in the caudal half of the ribcage near the vertebral column, contributing to a hotspot of injury that is centered on the thoracolumbar junction (Fig. 1.5b). With the exception of exhibiting a similar increase in pathology density in

the caudal rib cage, the distributions of dire wolf and sabertooth cat trauma are visually distinct. The dire wolf heat map clearly illustrates the concentrations of trauma on the anterior cervical vertebra and the limbs (distal humerus, proximal ulna and radius, mid-femur, distal tibia and fibula, and phalanges) (Figs. 1.5c, 1.6).

OHSA of *Smilodon* injuries found significant hotspots (CI>95%) in thoracic vertebrae medial to the scapula, posterior thoracic vertebrae and associated rib heads, anterior and middle lumbar vertebrae, and pes (Fig. 1.5b). In all cases except the pes, these results reinforce those of the statistical analysis. The pes is probably not a true hotspot, however. Its assignment as a hotspot more likely resulted from collapsing four metatarsals into a 2D image for spatial analysis (Fig. 1.5b). In the dire wolf, significant hotspots (CI>95%) were recovered in the anterior cervical vertebrae, mid-shaft of the femur, ankle, wrist, and metapodials, all bones where trauma frequencies were higher than expected (e.g. femur, tibia, fibula). No cold spots were detected in either species.

ANND analysis found that regions dominated by chronic muscle and joint injuries are more clustered than those with a greater proportion of healed fractures and blows, lending support to the injury diagnoses in regions such as the hindlimb (Fig. 1.6). Within the dire wolf, injury points were clustered in all areas except the lumbar region. The distance between points was less than half the expected distance (based on a random distribution) in the manus, pes, and cervical region Table 1.5). Injury locations in *Smilodon* were clustered in all regions except the cervical and lumbar vertebrae. The distance between neighboring points in the dire wolf hind limb and *Smilodon* cervical vertebrae was less than half of the expected, indicating highly clustered injuries.

DISCUSSION

Although detailed quantitative comparisons of injury type and frequency for extant pursuit (e.g. African wild dogs, *Lycaon pictus*) and ambush (e.g. African lions, *Panthera leo*) carnivorans are not available, there are data from other vertebrates that suggest that the most likely causes of injury include trauma incurred while pursuing and killing prey, and that injury rates might reflect hunting behavior. For example, three raptors that engage in high-speed pursuit of birds through the forest canopy (Cooper's hawks, sharp-shinned hawks, and goshawks) exhibited many more pectoral girdle fractures than species that hunt in open habitat (32,33). Similarly, a study of skeletal fracture rates in gray wolves and coyotes from Saskatchewan, Canada, found much higher rates of healed fractures in the wolves, a species that hunts relatively larger prey (34).

In the case of *Smilodon* and the dire wolf, most of the injuries probably occurred as a result of pursuing and killing prey rather than intra- and interspecific aggression, largely because the frequency of hunting activity is greater than that of dangerous predator-predator interactions. Moreover, the marked differences in the spatial distribution of trauma between the two species are better explained by hunting mode (ambush vs. pursuit) than battle wounds. Unlike healed fractures and evidence of trauma, which are clustered at muscle attachment sites or areas of structural weakness (e.g. mid-shafts of the ribs and limb bones), wounds – some specifically diagnosed as bites – are distributed more randomly (Fig. 1.4).

The greater absolute frequency of pathology in *S. fatalis* than *C. dirus* suggests that the former experienced a much greater risk of injury over its lifetime than the latter. Perhaps it is because they killed relatively larger prey (35) and may have done so at times as individuals, rather than in groups. Instead of exhausting their prey through a long pursuit, *Smilodon*

ambushed prey at a short distance and immobilized them using their massive forelimbs before killing them with precisely positioned bites (20-21,36). In addition to hunting behavior, it is possible that the overall higher incidence of injury in *Smilodon* could have resulted from a longer life span. Several studies of skeletal trauma have documented an increase in the probability of injury with age in primates and carnivorans (37-41). As of yet, it is not possible to assign individual age to isolated skeletal elements of adult sabertooths or dire wolves so we are unable to test for an effect of age. However, studies of dental wear in both *Smilodon* and the dire wolf at Rancho La Brea indicate that young adults of both species far exceed older individuals in the deposits (24,42). Consequently, the substantially higher frequency of injury in the La Brea sabertooth seems unlikely to be due to a longer average lifespan than dire wolves.

We predicted that dire wolves as pursuit predators would exhibit relatively more limb injuries than would the ambush predator, *Smilodon*. This was supported by higher than expected rates of trauma in the dire wolf across all limb bones and significant hotspots on the ankle and the mid-shaft of the femur. Like Ware (28), we found that most dire wolf injuries were repeated ligament and tendon re-injuries; our heat maps show increased density at major muscle and ligament attachment sites (Figs. 1.5, 1.6). Although there are no systematic reports of chronic injury in modern wild canids with which to compare this distribution, there are publications on pathology in extant herding, agility, and racing dogs (43-46) that support our hypothesis that tarsal, triceps, biceps femoris and gracilis injuries resulted from cursorial hunting.

By contrast, mapping *Smilodon* limb injuries produces clusters near sites of rotation such as the acetabulum (Fig. 1.6), caudal margins of the scapula, and lumbar vertebrae, supporting grappling as the method of subduing prey. Following an ambush, the sabertooth is believed to have used its robust forelimbs to wrestle its quarry to the ground with the hind feet planted on the

ground or against its prey (21,36,47). This would likely subject the shoulder girdle to strains while wrestling and the spinal column to twisting when the hind feet were planted. Consistent with this, the most frequent injuries were spinal, with trauma forming hotspots at T2, T10-L1, and L6-L7, respectively. Injury density and frequency are high across the entire lumbar region of *S. fatalis* with 20-50% of all vertebrae displaying traumatic pathology, most of which were attributed to torsion of the vertebrae relative to one another. When pulling prey to the ground, these vertebrae may have been subjected to rotational forces: T2 from the shoulder girdle and T13-L1 from the rotation of the thorax relative to the pelvis. While the shoulder joint itself was not an injury hotspot, trauma to attachment sites of the rotator cuff on the scapular margin and proximal humerus were observed in *Smilodon* but not in the dire wolf (Fig. 1.3).

Despite our prediction that dire wolf crania would be injured relatively often due to their close proximity to prey, the cranium was infrequently injured (1.6%, Table 1.1) and the dentary less so (0.18%, Table 1.1). However, despite the low frequency of dire wolf head injuries, the first three cervical vertebrae form an injury hotspot and are damaged more often than expected. This hotspot may result from strains incurred while holding or biting large ungulate prey given that neck muscles could act to constrain movements of the skull relative to the body caused by struggling prey. Among modern canids, African wild dogs were observed to be lifted off the ground while holding zebra by their muzzles (22) and gray wolves were seen being dragged by bison and moose that ran with the wolves latched on to their hindquarters (48). In contrast to the dire wolf, the cranium and anterior cervical region of *Smilodon* were injured much less than expected, with the cranium nearly devoid of traumatic injury. Based on the heat maps, *Smilodon* cervical injury density increases caudally, opposite to the pattern observed in the dire wolf. These contrasting patterns suggest that *Smilodon* was better able to protect the cranium

14

from trauma during prey capture. Such avoidance would have protected *Smilodon's* elongate canine teeth, which are fragile when subjected to mediolateral bending (42,49).

Spatial analysis of traumatic pathologies provided additional insights beyond those derived from the statistical analysis of the prevalence of pathologies. Spatial analyses enabled us to test our prediction that, relative to the dire wolf, the sabertooth cat would sustain more chest injuries due to forceful impacts with its prey. We found indirect evidence of chest impacts after the heat maps revealed patterns obscured by the disarticulation of skeletons at Rancho La Brea. Pathological rib heads adjoin injured costal facets primarily on the anterior thoracic vertebrae, suggesting that force was transmitted from the sternum to the head of the rib and subsequently to the vertebral column. This contributed to the overall high frequency of vertebral injury in *Smilodon* but left the ventral midline relatively uninjured. This is supported by a pattern seen in both species: in the first seven ribs, traumatic pathologies are concentrated at their proximal and distal ends whereas further posteriorly, where the ribs lack sternal reinforcement, mid-shaft fractures are the most common injury (Figure 1.4).

GIS is both a visualization and analysis tool. GIS visualization made the large volumes of injury data more accessible and easier to interpret in an anatomical context because it exposed hotspots of injury across joints such as the ankle and adjacent vertebrae (Fig. 1.5). Because we were able to quantify the distribution of injuries both within and across all elements, we could discriminate true hotspots from areas that appeared to be injury-dense using OHSA, and distinguish regions in which injuries were significantly clustered together using ANND analysis. ANND supported our diagnoses of chronic injury by identifying regions in which pathologies were clustered. If chronic injuries were diagnosed correctly, then those injury centroids would be expected to cluster at the attachments of muscles and at articular surfaces, whereas blows or

wounds would be less likely to occur in the same place on multiple individuals. Multiple pathologies on a single element were rare ($< 2\%$); thus, a clustered distribution and lower ANND ratio supports chronic pathology diagnoses.

In conclusion, there are clear and significant differences in the distribution and frequency of pathological elements in two large extinct carnivorans, *S. fatalis* and *C. dirus*. The markedly different distributions likely reflect the distinct hunting modes of these two species, while the difference in absolute frequency might be due to differing prey sizes and hunting behaviors.

Ideally, we would test these hypotheses using data on skeletal trauma in extant species with distinct hunting behaviors, such as gray wolves and lions. However, this requires large samples of post-cranial skeletal elements, which are rare in museums due to constraints on storing numerous large skeletons. Consequently, few reports examine non-pathological individuals to estimate the frequency of injury, and fewer still report pathologies in more than a handful of individuals (except for tooth fractures, e.g., ref. 25). Collaborative use of GIS among researchers in the field and in museums may be an ideal solution to the problems of storing skeletons and aggregating sporadic reports. Of course, the Rancho La Brea pathology collections are of unprecedented size and therefore allow for robust quantitative comparisons; nonetheless increased documentation of skeletal pathologies in both extant and extinct vertebrates using GIS technology could enhance our understanding of the significance of injury and disease in the lives of vertebrates, past and present.

TABLES AND FIGURES

Table 1.1. Element counts for CD (*Canis dirus*) and SF (*Smilodon fatalis*) used to determine MNI

ELEMENT	REGION	PATHOLOGIC AL CD	NON-PATH CD	TOTAL CD	PATHOLOGIC AL SF	NON-PATH SF	TOTAL SF	MNI
Skull	cranium	15	254	269	2	312	314	
dentary (rami)	cranium	70	547	617	5	225	230	
CV1	cervical	20	351	371	11	290	301	MNI CDI
CV2	cervical	13	310	323	7	300	307	
CV3	cervical	17	229	246	19	305	324	
CV4	cervical	6	247	253	10	287	297	
CV5	cervical	2	229	231	15	304	319	
CV6	cervical	8	234	242	14	275	289	
CV7	cervical	7	163	170	11	262	273	
TV1	thoracic	5	185	190	23	285	308	
TV2	thoracic	2	134	136	23	280	303	
TV3	thoracic	3	121	124	54	84	138	
TV4	thoracic	2	63	65	33	309	342	MNI SFA
TV5	thoracic	0	127	127	26	262	288	
TV6	thoracic	2	75	77	24	231	255	
TV7	thoracic	4	274	278	38	77	115	
TV8	thoracic	6	267	273	17	166	183	
TV9	thoracic	4	224	228	45	210	255	
TV10	thoracic	2	85	87	47	206	253	
TV11	thoracic	3	112	115	33	196	229	
TV12	thoracic	1	75	76	41	197	238	
TV13	thoracic	4	96	100	96	246	342	
L1	lumbar	9	162	171	87	41	128	
L2	lumbar	1	198	199	24	29	53	
L3	lumbar	3	241	244	29	50	79	
L4	lumbar	7	151	158	23	11	34	

L5	lumbar	5	281	286	30	28	58
L6	lumbar	3	195	198	39	46	85
L7	lumbar	16	198	214	31	43	74
Sacra(all)	pelvosacral	12	122	134	35	709	744
Innominate	pelvosacral	19	226	245	32	540	572
AntCauV	caudal	6	117	123	15	234	249
PosteriorCauV	caudal	2	NA	2	0	190	190
Rib 1	ribcage	10	322	332	11	NA	11
Rib 2	ribcage	2	264	266	8	NA	8
Rib 3	ribcage	0	197	197	2	NA	2
Rib 4	ribcage	2	340	342	6	NA	7
Rib 5	ribcage	0	214	214	2	NA	2
Rib 6	ribcage	2	170	172	8	NA	4
Rib 7	ribcage	3	164	167	0	NA	0
Rib 8	ribcage	3	167	170	10	NA	10
Rib 9	ribcage	11	224	235	13	NA	14
Rib 10	ribcage	5	247	252	25	NA	19
Rib 11	ribcage	11	207	218	14	NA	12
Rib 12	ribcage	4	300	304	24	NA	23
Rib 13	ribcage	9	252	261	17	NA	15
Rib, unidentified	ribcage	7	NA	7	4	NA	4
Sternebra	ribcage	1	NA	1	NA	NA	6
Manubrium	ribcage	2	NA	2	101	NA	7
Lumbar rib	developmental pathology	0	NA	0	4	NA	NA
Phalanges, unidentified	front and hind limb	32	1307	1339	18	14	32
scapula	front limb	4	120	124	37	394	431
Humerus	front limb	14	295	309	3	392	395
Radius	front limb	30	402	432	10	505	515
ulna	front limb	20	311	331	4	381	385
scapholunar	front limb	2	187	189	0	357	357
Pisiform	front limb	0	68	68	2	153	155
Trapezium	front limb	0	32	32	0	43	43
Trapezoid	front limb	0	0	0	0	30	30

Magnum	front limb	0	0	0	0	94	94
Unciform	front limb	0	27	27	0	157	157
MC1	front limb	0	34	34	1	122	123
MC2	front limb	3	511	514	7	397	404
MC3	front limb	9	516	525	6	385	391
MC4	front limb	13	550	563	3	370	373
MC5	front limb	12	478	490	1	379	380
1st carpal phalanx, digit I	front limb	NA	NA	NA	NA	134	134
1st carpal phalanx, digit II	front limb	NA	NA	NA	NA	255	255
1st carpal phalanx, digit III	front limb	NA	NA	NA	NA	259	259
1st carpal phalanx, digit IV	front limb	NA	NA	NA	NA	199	199
1st carpal phalanx, digit V	front limb	NA	NA	NA	NA	205	205
2nd carpal phalanx, digit II	front limb	NA	NA	NA	NA	108	108
2nd carpal phalanx, digit III	front limb	NA	NA	NA	NA	111	111
2nd carpal phalanx, digit V	front limb	NA	NA	NA	NA	65	65
femur	hind limb	43	209	252	14	667	681
patella	hind limb	0	NA	NA	5	NA	
tibia	hind limb	13	441	454	10	142	152
fibula	hind limb	4	121	125	11	450	461
calcaneus	hind limb	22	552	574	11	442	453
astragalus	hind limb	1	345	346	0	483	483
cuboid	hind limb	2	91	93	2	183	185
navicular	hind limb	1	62	63	6	NA	6
ectocuneiform	hind limb	1	12	13	2	86	88
cuneiform	hind limb	1	NA	1	0	1	1
MT1	hind limb	0	NA	0	3	4	7
MT2	hind limb	7	428	435	15	363	378

Element	Region								
MT3	hind limb		17	562	579		8	438	446
MT4	hind limb		12	563	575		10	459	469
MT5	hind limb		36	504	540		2	413	415
1st tarsal phalanx	hind limb	NA		1119	1119		5	259	264
1st tarsal phalanx, digit III	hind limb	NA	NA	NA	NA			59	59
1st tarsal phalanx, digit IV	hind limb	NA	NA	NA	NA			87	87
1st tarsal phalanx, digit V	hind limb	NA	NA	NA	NA			139	139
2nd tarsal phalanx	hind limb	NA		221	221	NA		171	171
2nd tarsal phalanx, digit III	hind limb	NA	NA	NA	NA			89	89
2nd tarsal phalanx, digit IV	hind limb	NA	NA	NA	NA			190	190
3rd tarsal phalanx	hind limb	NA		54	54	NA		NA	NA
Sesamoid	miscellaneous		0	5	5		0	242	242
Baculum	miscellaneous		1	77	78		0	NA	0
TOTALS			651	19565			1384	18106	

Table 1.2. Per Element Observed vs Expected Values. The expected number of elements with trauma was calculated using the null distribution (equal frequency of injury to all elements) and a G test of independence. A significant difference (p<.05) from the null distribution within each species is indicated with asterisks and bold type. CDI, *Canis dirus*. SFA, *Smilodon fatalis*.

Element	Observed CDI	Expected CDI	Non-path	Sig. Within Species	Observed SFA	Expected SFA	Non-path	Sig. Within Species
CV1	17	14	351	*	2	17	290	*
CV2	13	12	310		4	18	300	
CV3	17	9	229	*	8	18	305	
CV4	4	10	247		6	17	287	
CV5	2	9	229		5	18	304	
CV6	8	9	234		4	16	275	
CV7	6	6	163		5	16	262	
TV1	2	7	185		13	17	285	
TV2	1	5	134		11	17	280	
TV3	3	5	121		9	5	84	*
TV4	2	3	75		7	19	309	
TV5	0	5	127		8	16	262	
TV6	1	3	75	*	13	14	231	
TV7	1	12	308	*	10	5	77	*
TV8	3	10	267		4	10	166	
TV9	3	9	224		15	13	210	*
TV10	1	3	85		23	13	206	*

TV11	1	4	112		**23**	**13**	**196** *
TV12	1	6	164		**31**	**13**	**197** *
TV13	2	8	209		**71**	**19**	**246** *
L1	6	6	162		**30**	**5**	**59** *
L2	1	8	198		**16**	**3**	**42** *
L3	**0**	**9**	**241** *		**19**	**2**	**72** *
L4	2	6	151		**13**	**2**	**16** *
L5	3	11	281		**28**	**4**	**40** *
L6	2	7	195		**26**	**5**	**66** *
L7	8	8	198		**11**	**4**	**62** *
Sacrum	24	15	366		19	44	728
Innominate	**16**	**11**	**266** *		27	33	540
Femur	**37**	**9**	**209** *		11	25	414
Tibia	**39**	**17**	**420** *		**9**	**9**	**142** *
Fibula	**29**	**16**	**394** *		13	15	248
Scapula	2	5	120		**27**	**16**	**247** *
Humerus	**13**	**12**	**295** *		**2**	**31**	**521** *
Radius	**29**	**16**	**402** *		10	15	240
Ulna	**20**	**13**	**311** *		3	5	89
Skull	9	10	254		**1**	**18**	**312** *

Table 1.3. Sample size for each element and the percent that exhibited trauma for *Smilodon* (SFA) and *C. dirus* (CDI). A proportions test was used to test for significant difference between the two species. Significance is indicated with asterisks and bold type.

Element	SFA % Trauma	CDI % Trauma	Significance Between Species
CV1	**0.7%**	**4.8%**	*
CV2	**1.3%**	**4.2%**	*
CV3	2.6%	7.4%	
CV4	**2.1%**	**1.6%**	*
CV5	1.6%	0.9%	
CV6	1.5%	3.4%	
CV7	1.9%	3.7%	
TV1	4.6%	1.1%	
TV2	3.9%	0.7%	
TV3	**10.7%**	**2.5%**	*
TV4	2.3%	2.7%	
TV5	3.1%	0.0%	
TV6	5.6%	1.3%	
TV7	**13.0%**	**0.3%**	*
TV8	2.4%	1.1%	
TV9	**7.1%**	**1.3%**	*
TV10	**11.2%**	**1.2%**	*
TV11	**11.7%**	**0.9%**	*
TV12	**15.7%**	**0.6%**	*

TV13	**28.9%**	**1.0%**	*
L1	**50.8%**	**3.7%**	*
L2	**38.1%**	**0.5%**	*
L3	**26.4%**	**0.0%**	*
L4	**81.3%**	**1.3%**	*
L5	**70.0%**	**1.1%**	*
L6	**39.4%**	**1.0%**	*
L7	**17.7%**	**4.0%**	*
Sacrum	2.6%	6.6%	
Innominate	5.0%	6.0%	
Femur	**2.7%**	**17.7%**	*
Tibia	**6.3%**	**9.3%**	*
Fibula	5.2%	7.4%	
Scapula	**10.9%**	**1.7%**	*
Humerus	**0.4%**	**4.4%**	*
Radius	4.2%	7.2%	
Ulna	3.4%	6.4%	
Skull	0.3%	3.5%	

Table 1.4. Percentage of traumatic pathology by region.

	S. fatalis		*C. dirus*	
	Total # pathological elements	% of total	Total # pathological elements	% of total
Skull and dentary	**2**	**<1**	**10**	**1.8**
Vertebral Column				
Cervical	34	4.4	67	12.1
Thoracic	231	29.8	21	3.8
Lumbar	143	18.4	22	4.0
Sacral	8	<1	5	1
Caudal	15	2	4	<1
Total Vertebrae	**431**	**56**	**119**	**21.6**
Forelimb				
Scapula	27	3.5	2	<1

Humerus, radius, Ulna	15	2	62	11.2
Manus	37	4.8	61	11
Total Forelimb	**79**	**10.2**	**125**	**22.6**
Hindlimb				
Innominate	21	2.7	12	2.2
Femur, Patella, Tibia, Fibula	37	4.8	105	19.0
Pes	62	7.7	118	21.3
Total Hindlimb	**120**	**12.5**	**235**	**42.4**
Ribcage	131	16.9	63	11.4
Sternum	13	1.7	2	<1
	144	**19**	**65**	**11.7**
Total Skeleton	776	99.7	554	100

Table 1.5. Average Nearest Neighbor Distance ratio and statistics. A distance ratio of 1 indicates

a perfectly even distribution over the defined region, while values <1 indicate clustered points.

	Distance				
S. fatalis	Ratio	Z	p	Count	Cluster
Hindlimb	0.37881	-4.12994	0.85967	37	most
Thoracic	0.531956	-14.1858	0	231	
Pes	0.612903	-5.7834	0	62	
Pelvic/Sacral	0.636175	-6.72249	0.85967	29	
Manus	0.663279	0.000173	0	34	
Forelimb	0.678185	-4.12994	0.000036	42	
Rib	0.866324	-3.07942	0.002074	144	least
Cervical	1.003	0.041049	0.967257	34	random
Lumbar	1.017	0.373243	0.708968	143	
Cranium	NA			2	

	Distance				
C. dirus	Ratio	Z	p	Count	Cluster
Pes	0.34106	-13.577	0.000001	118	most
Manus	0.38934	-9.9126	0.000001	61	
Cervical	0.481942	-8.29199	0	67	
Cranium	0.599227	-3.25286	0.001	10	

Rib	0.6698	-5.1305	0.000001	65	
Forelimb	0.69931	-4.778	0.000002	64	
Thoracic	0.769105	-2.0718	0.0382	21	
Hindlimb	0.87817	-2.889	0.003859	105	
Pelvic/Sacral	0.9842	-0.131	0.8955	17	least
Lumbar	1.02	10.01	0	22	random

Figure 1.1. Examples of common chronic pathologies in *Canis dirus* and *Smilodon fatalis*. (a) Ventral view of a pathological dire wolf atlas with bony growths indicative of chronic muscle injury on the left wing and osteoarthritic deposits at the atlanto-axial joint. (b) Non-pathological atlas of C. dirus. (c) Dorsal view of torsion injuries to 8th-12th thoracic vertebrae from a single *Smilodon*. Asymmetrical articulations between vertebrae have been outlined in white for ease of viewing. The neural spine of T11 (outline and arrow) is reduced in size and set at an unusual angle. (d) Non-pathological 8th-12th vertebrae of a single *Smilodon*.
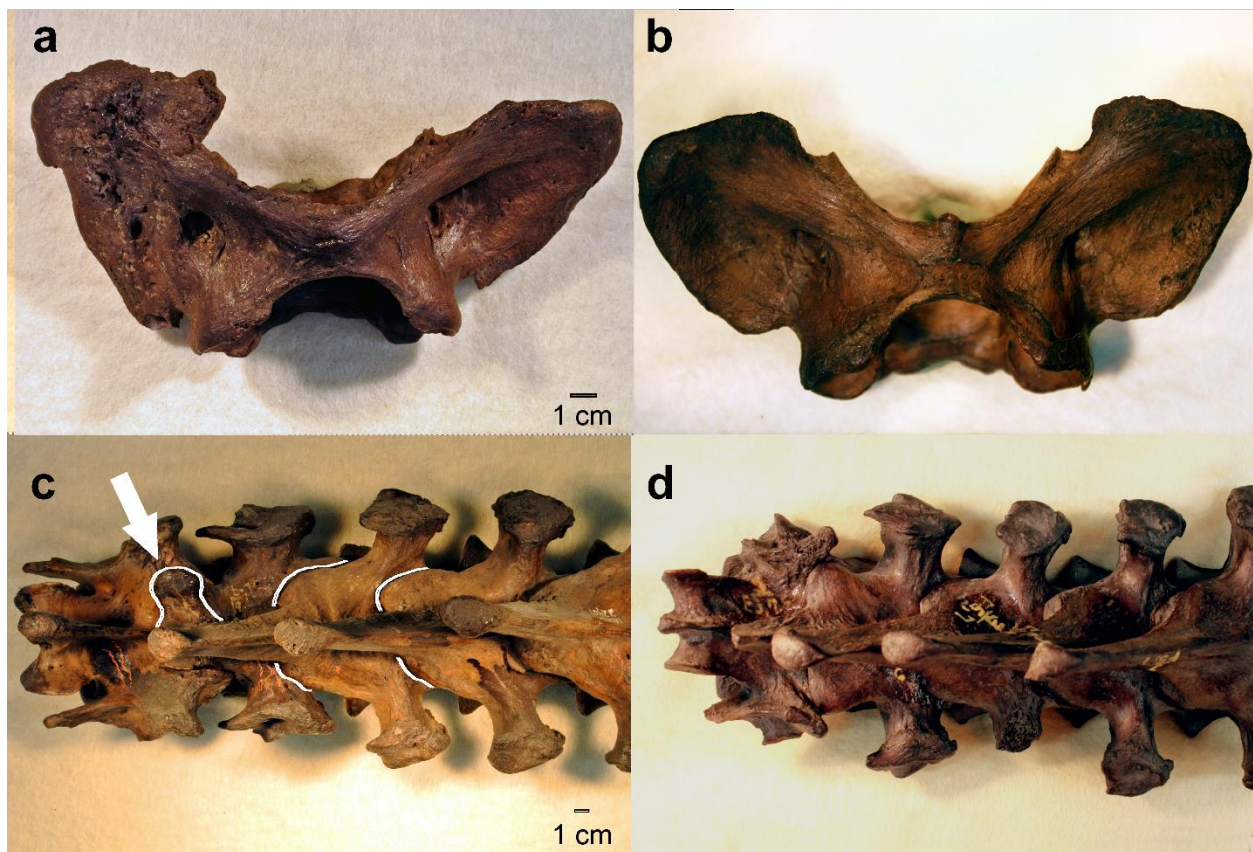
Figure 1.2. Observed (light blue) and expected (dark gray) counts of pathological elements by anatomical region in *Smilodon* and *Canis dirus*. Regions are shaded gray or white and coded as follows: 1, cranium and cervical vertebrae; 2, thoracic vertebrae; 3, lumbar vertebrae; 4, sacrum and innominate; 5, hindlimb; 6, forelimb. The percentage of traumatic and chronic injuries per region is given above the bars (see Table 3.4). Asterisks indicate a significant difference (p<.05) between the observed and expected counts for that element. Sample sizes for each element are in Table 1.1.
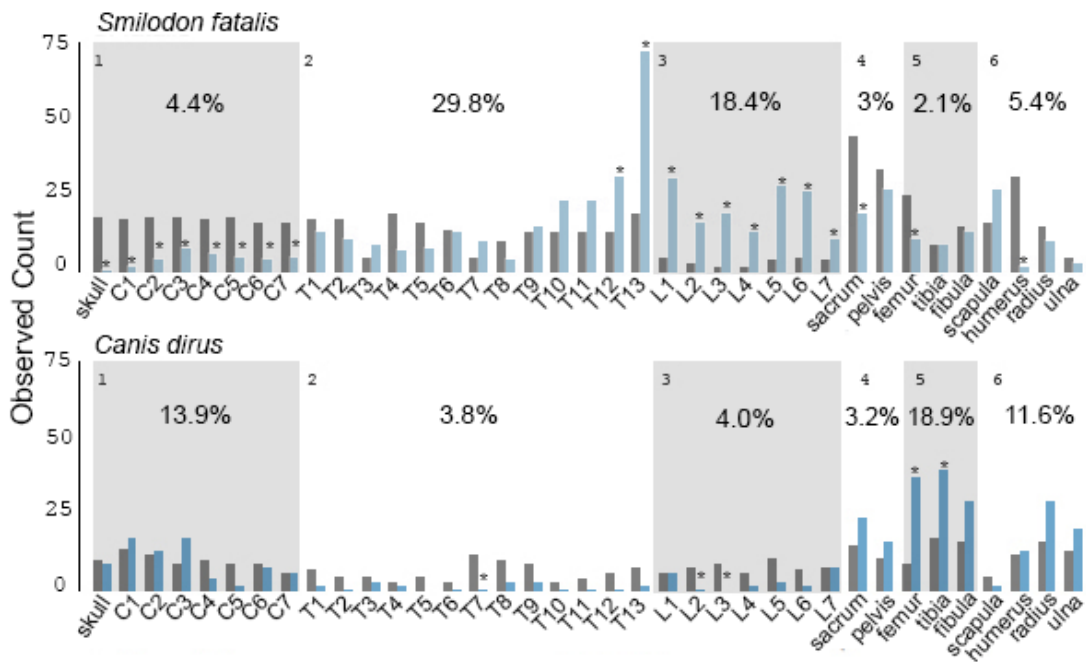
Figure 1.3. Digitization of skeletal pathologies. (A) All Pit 61/67 *Smilodon* scapular injuries colored by injury type. The centroids of traumatic injury are represented dots above the polygon layer. The dark red polygon, an example of calcified hematoma (myositis ossificans) labelled 8196, was digitized from photograph (B). All injuries were mapped onto the left side of the skeleton, thus the injured portion of 8196, a right scapula, appears mirrored. Missing portions of specimen 8196 were caused by post-mortem damage.
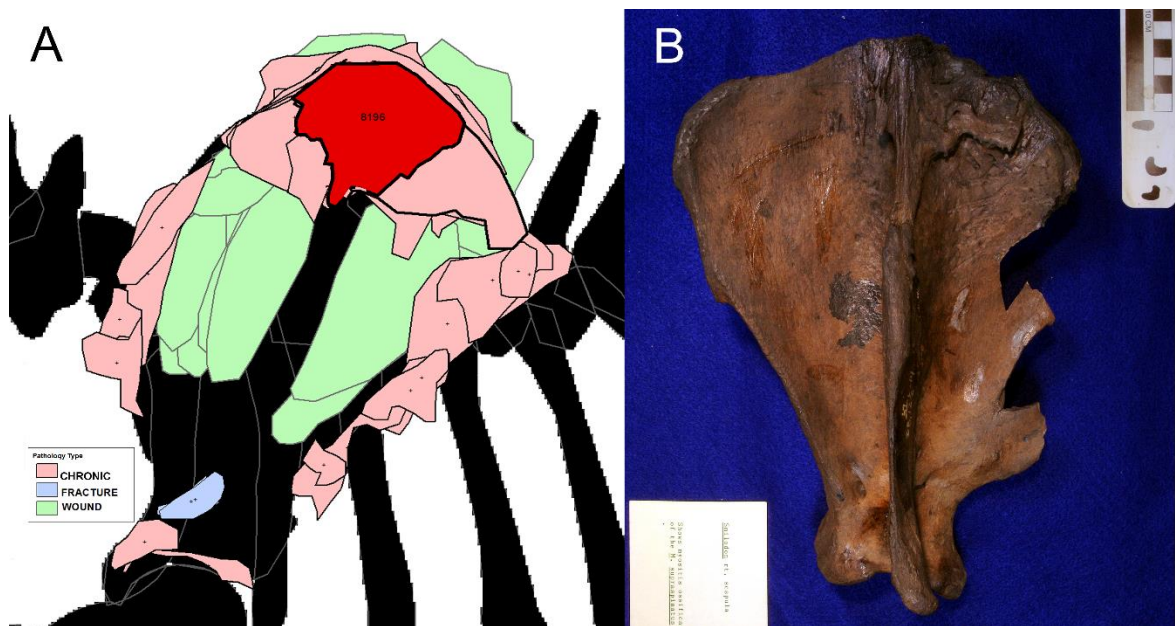
Figure 1.4. Polygonal representations of pathologies filtered to show only healed fractures, infected wounds and traumatic injuries. Wound distribution is not included in traumatic pathology analysis. Wounds are not considered putative hunting injuries because they are likely to be caused by a variety of other behaviors, such as lacerations from environmental hazards and conflict with other carnivorans. SF base map adapted from Harris, John M., and George T. Jefferson, eds. *Rancho La Brea: treasures of the tar pits*. No. 31. Natural History Museum of Los Angeles County, 1985. CD base map adapted from Stock, Chester, and John Michael Harris. *Rancho La Brea: a record of Pleistocene life in California*. No. 37. Natural History Museum of Los, 1992.

Smilodon fatalis- Wounds

n=59

Smilodon fatalis- Fractures
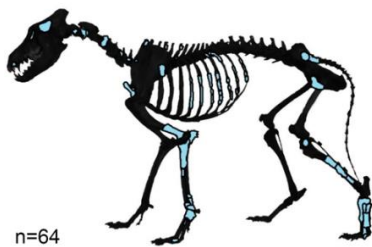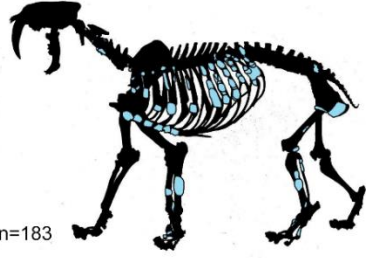
n=183

Smilodon fatalis- Trauma (Chronic+Fractures)
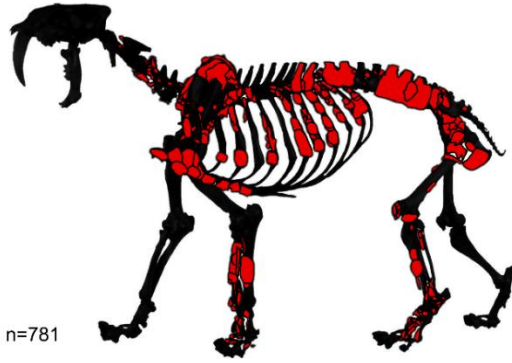
n=781

Figure 1.5. Distribution of traumatic and chronic pathology centroids across (a) *Smilodon fatalis* and (c) *Canis dirus* skeletal "base maps". All pathologies are visualized in a single plane from the lateral view regardless of location (i.e. pathologies on the lateral and medial aspect of an element are both shown and not distinguished). Note also that pathologies on vertebrae behind the scapula or innominate are seen through the overlying bones. More intense colors represent higher point density. Density measures are unitless. Map units are not equal between dire wolf and *Smilodon* maps, thus color intensity does not represent the same density across maps. (b and d) Optimized Hot Spot Analysis (OHSA) of pathology centroids show areas of pathology density that are significantly higher than the average for each species, colored by confidence interval. No cold spots were detected. SF base map adapted from Harris, John M., and George T. Jefferson, eds. *Rancho La Brea: treasures of the tar pits*. No. 31. Natural History Museum of Los Angeles County, 1985. CD base map adapted from Stock, Chester, and John Michael Harris. *Rancho La Brea: a record of Pleistocene life in California*. No. 37. Natural History Museum of Los, 1992.
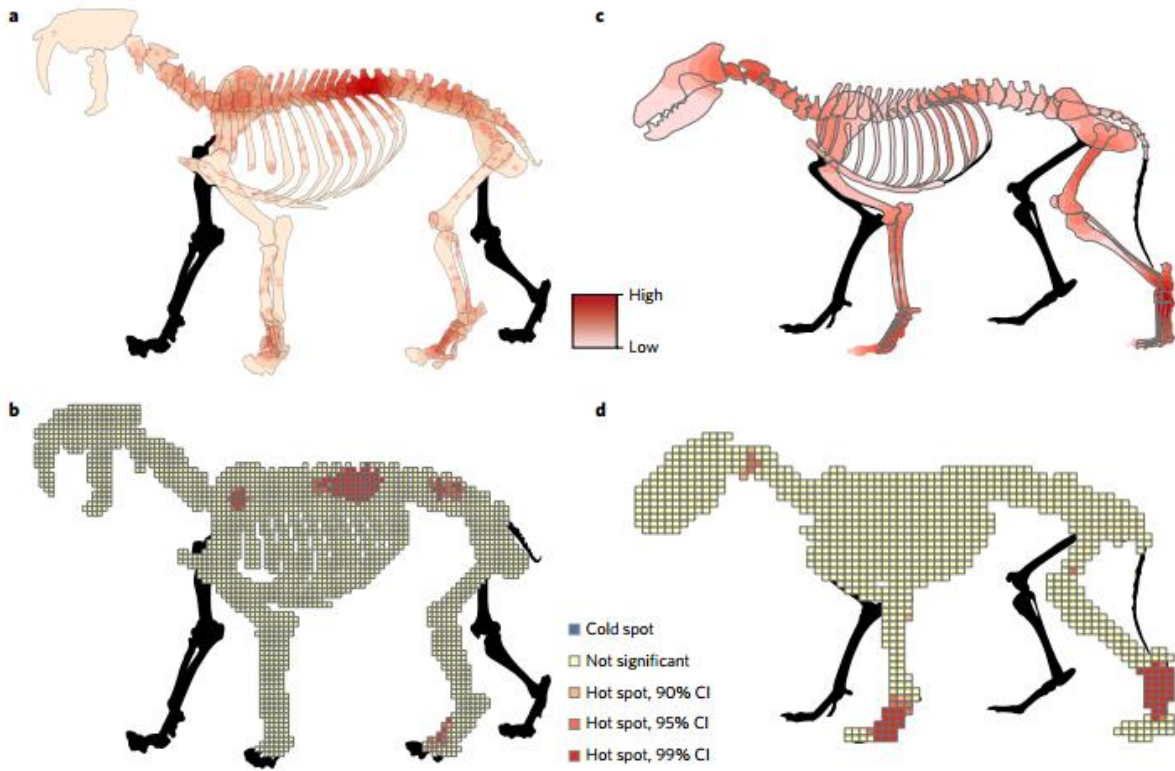
Figure 1.6. Density/heat map depictions of traumatic and chronic pathology centroids across a *Smilodon fatalis* (left) and *Canis dirus* (right) hindlimb. All pathologies are visualized in a single plane from the lateral view. Smaller symbols represent pathologies on the medial aspect of the limb. Warmer colors represent higher point density. Density measures are unit-less. Map units are not equal between dire wolf and *Smilodon* maps; thus color intensity does not represent the same density across maps. (a1)- Articulation between ilium and sacrum. Origin of deep gluteal m. (b1), (c1)- Patellar portion of the quadriceps femoris tendon. (d1, e1)- Attachments of joint-stabilizing ligaments. (a2)- Origin of superficial gluteal mm. (b2)- Origin of hamstring muscle group. (c2)- Insertion of adductor muscle group. (d2) Origin of gastrocnemius and superficial digital flexor mm. (e2)-Location of intratarsal joints and passage of the digital flexor tendon.
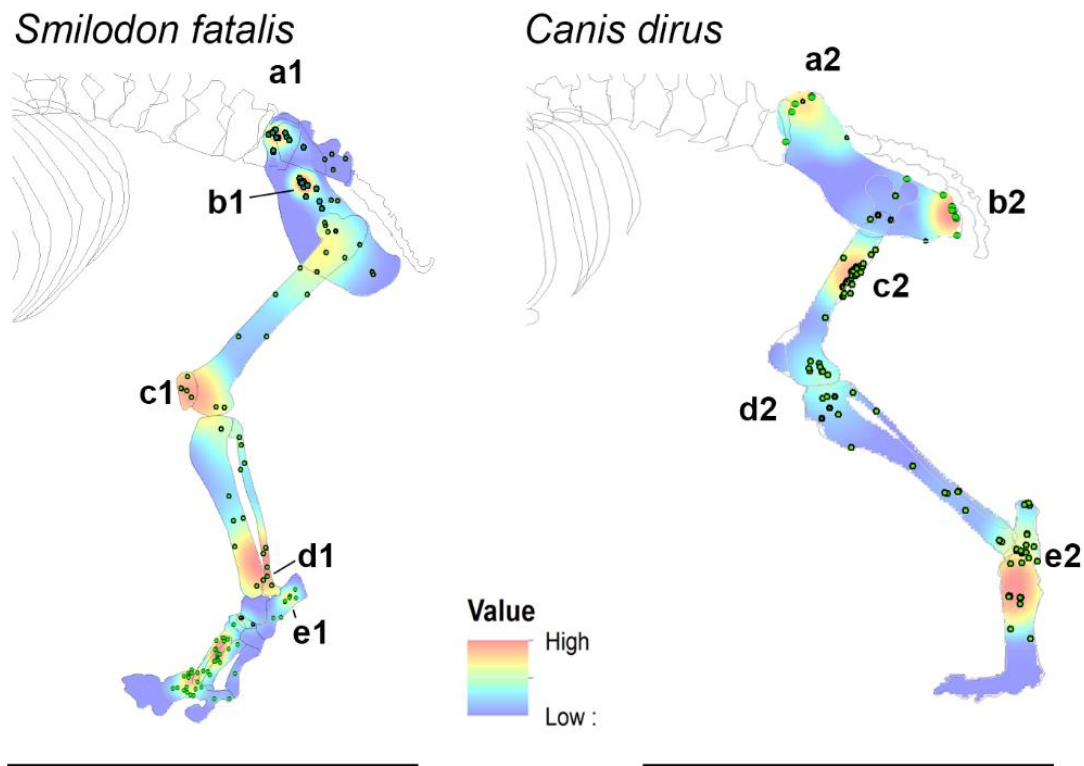
REFERENCES

1. Stewart, T. in *The First Americans: Origins, Affinities, and Adaptations* (eds Laughlin, W. & Harper, A.) 257–274 (Fischer, 1979).

2. Jurmain, R.D. The pattern of involvement of appendicular degenerative joint disease. *Am. J. Phys. Anthropol.* **53,** 143–150 (1980).

3. Bridges, P.S. Prehistoric Arthritis in the Americas. *Annu. Rev. Anthropol.* **21,** 67–91 (1992).

4. Bridges, P.S. Vertebral arthritis and physical activities in the prehistoric southeastern United States. *Am. J. Phys. Anthropol.* **93,** 83–93 (1994).

5. Berger, T.D. & Trinkaus, E. Patterns of trauma among the Neandertals. *J Archaeol. Sci.* **22,** 841–852 (1995).

6. Carbone, C., Teacher, A., & Rowcliffe, J.M. The costs of carnivory. *PLoS Biol.* **5,** 363–368 (2007).

7. Mukherjee, S. & Heithaus, M.R. Dangerous prey and daring predators: a review. *Biol. Rev.* **8,** 550-563 (2013).

8. Stock, C. *Rancho La Brea: A Record of Pleistocene Life in California*, 7th edn (Natural History Museum of Los Angeles County, 1992).

9. Fuller, B. T., Harris, J. M., Farrell, A. B., Takeuchi, G. T., & Southon, J. R. Sample preparation for radiocarbon dating and isotopic analysis of bone from Rancho La Brea. *Natural History Museum of Los Angeles County Science Series*, **42,** 151–167 (2015).

10. Herrmann, N. GIS applied to bioarchaeology: an example from the Rio Talgua caves in Northeast Honduras. *Cave and Karst Studies* **64**, 17–22 (2002).

11. Jennings, D.S. & Hasiotis, S.T. Taphonomic analysis of a dinosaur feeding site using geographic information systems (GIS), Morrison Formation, southern Bighorn Basin, Wyoming, USA. *Palaios* **21**, 480–492 (2006).

12. Marean, C.W., Abe, Y., Nilssen, P.J., & Stone, E.C. Estimating the minimum number of skeletal elements (MNE) in zooarchaeology: a review and a new image-analysis GIS approach. *Am. Antiquity* **66,** 333–348 (2001).

13. Parkinson, J.A. A GIS Image Analysis Approach To Documenting Oldowan Hominin Carcass Acquisition: Evidence From Kanjera South, FLK Zinj, And Neotaphonomic Models Of Carnivore Bone Destruction (doctoral dissertation, City University of New York, 2013).

14. Parkinson, J.A., Plummer, T.W., & Bose, R. A GIS-based approach to documenting large canid damage to bones. *Palaeogeog. Palaeoclim. Palaeoecol.* **409**, 57–71 (2014).

15. Parkinson, J.A., Plummer, T.W., & Hartstone-Rose, A. Characterizing felid tooth marking and gross bone damage patterns using GIS image analysis: an experimental feeding study with large felids. *J. Human Evol.* **80,** 114–134 (2015).

16. Garb, J.L., Ganai, S., Skinner, R., Boyd, C.S., & Wait, R.B. Using GIS for spatial analysis of rectal lesions in the human body. *Int. J. Health Geogr.* **6,** 11, doi:10.1186/1476-072x-6-11 (2007).

17. Andersson, K., & Werdelin, L. The evolution of cursorial carnivores in the Tertiary: implications of elbow-joint morphology. *Proc Roy Soc B.* **270,** S163-S165 (2003).

18. Figueirido, B., Martín-Serra, A., Tseng, Z.J., & Janis C.M. Habitat changes and changing predatory habits in North American fossil canids. *Nature Comm.* **6**, doi:10.1038/ncomms8976 (2015).

19. Gonyea, W. J. Behavioral implications of saber-toothed felid morphology. *Paleobiol.* **2,** 332–342 (1976).

20. Anyonge, W. Locomotor behavior in Plio-Pleistocene saber-tooth cats: a biomechanical analysis. *J. Zool. (Lond).* **238,** 395–413 (1996).

21. Antón, M. *Sabertooth* (Indiana Univ Press, 2013).

22. Malcolm, J.W., & Van Lawick, H. Notes on wild dogs (*Lycaon pictus*) hunting zebras. *Mammalia.* **39,** 231-240 (1975).

23. Mech, L.D. *Wolf* (Doubleday, 2012).

24. Binder, W.J., Thompson, E.N., & Van Valkenburgh, B. Temporal variation in tooth fracture among Rancho La Brea dire wolves. *J. Vert. Paleontol.* **22,** 423–428 (2002).

25. Van Valkenburgh, B. Costs of carnivory: tooth fracture in Pleistocene and Recent carnivorans. *Biol. J. Linn. Soc.* **96,** 68–81 (2009).

26. Hartstone-Rose A., Dundas R.G., Boyde B., Long R.C., Farrell A.B., & Shaw C.A. The bacula of Rancho La Brea. *Natural History Museum of Los Angeles County Science Series*, **42**, 53-64 (2015).

27. Scott, E., Rega, E., Scott, K., Bennett, B., & Sumida, S. A pathological timber wolf (*Canis lupus*) femur from Rancho La Brea indicates extended survival after traumatic amputation injury. *Natural History Museum of Los Angeles County Science Series*, **42,** 33-36 (2015).

28. Ware, S. Disease, Skeletal Injury And Trauma As Possible Behavior Modifiers In The Fossil Dire Wolf Canis Dirus (Canidae: Carnivora) From Rancho La Brea, California (Doctoral dissertation, Union Institute and University, 2005).

29. Rothschild, B.M. & Martin, L.D. in *The Other Saber-Tooths: Scimitar-Tooth Cats Of The Western Hemisphere* (eds Naples, V.L., Martin, L.D., & Babiarz, J.P.) 35–41 (Johns Hopkins University Press, 2011).

30. Heald, F., Shaw, C. in *Great Cats. Majestic Creatures of the Wild* (eds. Seidensticker, J. & Lumpkin S.) 26–27 (Rodale Press, 1991).

31. Shaw C.A. Old wounds: the paleopathology of Rancho La Brea. *Terra* **31,** 17 (1992).

32. Bedrosian, B.E., & St. Pierre, A.M. Frequency of injury in three raptor species wintering in northeastern Arkansas. *Wilson J. Ornithol.* **119,** 296–298 (2007).

33. Roth, A.J., Jones, G.S., & French, T.W. Incidence of naturally healed fractures in the pectoral bones of American accipiters. *J. Raptor Res.* **36,** 229–230 (2002).

34. Wobeser, G. Traumatic, degenerative, and developmental lesions in wolves and coyotes from Saskatchewan. *J. Wildl. Diseases* **28,** 268–275 (1992).

35. Van Valkenburgh, B, Hayward, M.W., Ripple, W.J., Meloro, C., & Roth V.L. The impact of large terrestrial carnivores on Pleistocene ecosystems. *PNAS.* **113,** 862-867 (2016).

36. Akersten, W.A. Canine function in *Smilodon* (Mammalia: Felidae: Machairodontidae). Contributions in Science (Los Angeles). **356,** 1–22 (1985).

37. Bramblett, C.A. 1967 Pathology in the Darajani baboon. *Am. J. Phys. Anthropol.* **26,** 331–340.

38. Buikstra, J.E. Healed fractures in *Macaca mulatta*: age, sex and symmetry. *Folia Primatol.* **23,** 140–148 (1975).

39. Harris, S. Injuries to foxes (*Vulpes vulpes*) in suburban London. *J. Zool.* **186,** 567–572 (1978).

40. Kano, T. Observations of physical abnormalities among the wild bonobos (*Pan paniscus*) of Wamba, Zaire. *Am. J. Phys. Anthropol.* **63,** 1–11 (1984).

41. Wilkins, L., Allen, J.M., Coltrain, J., Flanagin, A., Allen, T.D., & Reed, D.L. Methods of assessing health and diet of Florida panthers (*Puma concolor*) using museum specimens. Part 1. Osteology as a means of assessing Florida panther health. *Bull. Florida State Mus. Nat. Hist.* **47,** 74-98 (2007).

42. Van Valkenburgh, B. & Hertel, F. Tough times at La Brea: tooth breakage in large carnivores of the late Pleistocene. Science **261,** 456–459 (1993).

43. Marcellin-Little, D.J., Levine, D., Taylor, R. Rehabilitation and conditioning of sporting dogs. *Vet. Clin. North Amer.: Small Anim. Practice.* **35,** 1427–1439 (2005).

44. Davis, P.E. Toe and muscle injuries of the racing greyhound. *NZ Veter. J.* **21,** 133–146 (1973).

45. Worth, A.J., Danielsson, F., Bray, J.P., Burbidge, H.M., & Bruce, W.J. Ability to work and owner satisfaction following surgical repair of common calcaneal tendon injuries in working dogs in New Zealand. *NZ Vet. J.* **52,** 109–116 (2004).

46. Vaughan, L.C. Gracilis muscle injury in greyhounds. *J. Small Anim. Practice.* **10,** 363–375 (1969).

47. Meachen-Samuels, J.A. & Van Valkenburgh B. Radiographs reveal exceptional forelimb strength in the sabertooth cat, *Smilodon fatalis*. *PLoS ONE* **5**:e11412, doi:10.1371/journal.pone.0011412 (2010).

48. Carbyn, L.N., Oosenbrug, S., Anions, D.W. *Wolves, bison and the dynamics related to the Peace-Athabasca Delta in Canada's Wood Buffalo National Park* (Canadian Circumpolar Institute Press, 1993).

49. Van Valkenburgh, B. & Ruff, C.B. Canine tooth strength and killing behaviour in large carnivores. *J. Zool.* **212,** 379–397 (1987).

50. White T.E. A method of calculating the dietary percentage of various food animals utilized by aboriginal peoples. *Am. Antiq.* **18,** 396–398 (1953).

51. How Optimized Hot Spot Analysis Works—ArcGIS Pro | ArcGIS for Desktop. ArcGIS Pro | ArcGIS for Desktop. (http://pro.arcgis.com/en/pro-app/tool-reference/spatial-statistics/how-optimized-hot-spot-analysis-works.htm)

52. How Average Nearest Neighbor Distance (Spatial Statistics) works. ArcGIS Resources. (http://resources.esri.com/help/9.3/ArcGISDesktop/com/Gp_ToolRef/spatial_statistics_tools/how_average_nearest_neighbor_distance_spatial_statistics_works.htm)

53. White T.E. A method of calculating the dietary percentage of various food animals utilized by aboriginal peoples. Am. Antiq. 18, 396–398 (1953).

CHAPTER 2

Skeletal and Dental Development Preserves Evidence of Population Fluctuations in the Moose of Isle Royale

INTRODUCTION

In archeological and paleontological mammalian samples, the health of individuals can be read from episodes of arrested skeletal growth. Mammalian teeth and skeletons contain a wealth of information about the life history of individuals and can thus preserve information about populations. Slowed or interrupted growth results from severe metabolic stress, such as might occur in association with an individual's birth, weaning, episodes of disease, and poor nutrition. To test whether skeletal features track changes in population density, we chose ungulates, the prey base of most human societies and terrestrial large mammal ecosystems for the past 50 million years. Ultimately, we hope to complement existing methods of estimating carnivoran[1] and proboscidean[2] population changes from skeletal material, allowing better characterization of Holocene and Anthropocene ecosystems. Such an approach requires skeletal characters that can be sampled non-destructively and have a high probability of surviving taphonomic processes. We identified such characters using skeletal material from a well-characterized, self-contained moose (*Alces alces*) population inhabiting Isle Royale National Park, Michigan.

Isle Royale, a 544 km^2 island in Lake Superior, was colonized by moose early in the twentieth century via a rare ice bridge. Isolated 90km off the shore of Ontario, the moose population is unique in that both immigration and emigration are negligible and there is only a single predator, the wolf, which contributes to moose mortality. These properties have allowed the moose

population to cycle through drastic expansions and contractions. Over the past 58 years, this isolated predator-prey system has been meticulously documented, facilitating assessment of the effects of climate, population size, and predation on ungulate health and mortality Throughout this time period, Isle Royale's minimal moose population has exceeded that of mainland areas, which often fall below 0.03 moose/km^2 [IRNP minimum 0.71; Mainland mean 0.55 +-.647] (3) . Resource limitation due to these elevated densities is putatively the mechanism driving the rapid dwarfing of the now century-old Isle Royale moose population (4,5)given that it has been shown to decrease carcass weight in multiple North American moose populations(6).

Studies of several populations have suggested that a variety of skeletal anomalies accompany poor juvenile nutrition in cervids. For example delayed tooth emergence(7), shortened metatarsal bones(4,5,8), osteoarthritis(9), and osteoporosis(10) have all been linked to malnutrition. Mandible length is of particular interest as the mandible has a high growth priority over other bones shortly after birth and slows only in the second year of life(11). Prior to the dramatic population crash of 1996, shortened mandibles were suggested to be linked to elevated population densities on Isle Royale(12) as they have in caribou(13). However a study of female moose(6) found that growth rate, not final size, was affected. Climate also has a significant effect on moose osteological development(5,14) and the Isle Royale population's growth rate(14) and thus may be expected to play a role in the new characters assessed here.

It has been suggested that developmental defects of tooth enamel could be used to track ungulate population irruptions(15), but tooth tissue's capacity for preserving historical population density changes has not been tested. The permanent dentition is a prime candidate for preserving

evidence of irruptions because tooth tissue does not remodel. The crowns of moose permanent

cheek teeth form in a period that spans approximately one year from roughly 3 months before

birth to 6-8 months post-weaning(16) (Figure 2.1). Thus, malnutrition may affect the

development of tooth enamel both directly, through lack of forage and indirectly, through an

inadequately nourished mother. If foraging juveniles are insufficiently nourished, the

development of enamel will be slowed and or interrupted, leaving diagnostic features that will

persist into adulthood. In the laboratory and in domesticated animals, caloric restriction produces

arrested bone growth (i.e. LAGs), delayed tooth eruption, malocclusion, changes in mandibular

shape, and dental enamel hypoplasias(17). Dental enamel hypoplasias (DEH) are among the

most conspicuous, manifesting as a localized thinning or absence of enamel visible to the naked

eye(18,19). DEH are caused by impaired enamel secretion, a symptom of severe

nutritional(17,20), pathological(18,21–23)or environmental stress(15,24–28). The morphology of

DEH can vary with the degree of metabolic stress (29), but DEH are easily identified in

ungulates with exposed enamel surfaces, such as moose. In extant and extinct wild ungulates,

hypoplasias have been attributed to weaning and seasonal stressors in giraffids (*Giraffa,*

Sivatherium)(25,26); bison (*Bison bison*)(27,28,30) white deer (*Odocoileus virginianus*(31)) and

caribou (*Rangifer tarandus groenlandicus*)(15).

To create a method broadly applicable to archeological and paleontological samples, we focus on

the size of two skeletal elements that are often preserved, mandibles with teeth and

metapodials(32). In addition, we quantified the frequency of growth anomalies (DEH) in the

enamel of the cheek teeth. When compared to animals weaned in low-density years, moose that

develop during periods of high population density are predicted to exhibit higher frequencies of

anomalies in tissues that form after weaning (enamel, mandibular bone) in addition to shortened stature. This is the first study of developmental defects in tooth enamel in a wild population spanning several decades, climate changes and population regimes.

METHODS

Materials

Skeletal specimens of moose collected from Isle Royale National Park (IRNP) are housed in the Michigan Technical Institute Mooseum in Alberta, Michigan. Moose with associated mandibles and metatarsal bones were preferentially sampled. IRNP samples have been aged using cementum annuli, allowing each to be assigned a birth year. For 20 IRNP mandible specimens without cementum ages we imputed the period in which the animal was born based on the specimen's autopsy number and age at death. IRNP mandible and metatarsus length were shared by the Isle Royale Wolf Project and Isle Royale climate and moose density data were downloaded from the Isle Royale Wolf Project website (isleroyalewolf.org). We also compared mandibles from IRNP moose to those from the closest mainland Ontario population. The mainland sample (hereafter abbreviated as ONT) spanned the period 1950-1970, and thus experienced the same climate conditions as our earliest IRNP low density study period (1959-1963). ONT specimens are housed at the Royal Ontario Museum in Toronto, Canada. Population density of the ONT population was estimated using Canadian Department of Lands and Forests survey data and maps provided by the Canadian Ministry of Wildlife. To assess the impact of population density on skeletal characters, we analyzed data on mandible length (IRNP

n=906; ONT n=36), metatarsus length (IRNP n=62), and enamel hypoplasias (IRNP n=65, ONT n=71).

Population density threshold

Previous work has suggested that a density greater than two moose per km^2 (total island population equal to 1,071) may result in stunted bone growth, particularly in the length of the mandible(12). In addition, the carrying capacity of the island, as determined by browse availability surveys made between 1945 and 1970, was estimated to be 1000 moose (or 1.83 moose/km^2). We used the average of these two density estimates (1.92) as the density threshold beyond which moose are expected to show evidence of stress. Overpopulation and resource limitation can impact moose growth during the year they are born, or during gestation, or perhaps even two years before because moose population growth has been linked to the density of forage two years prior[34].To determine which of the three possible years (birth, gestation, two years prior to birth) to use as the one that defines whether an individual is classified as subject to high or low density conditions, we explored correlations between each candidate year and the length of the mandible and DEH. We explored the correlations between population size, DEH and mandible length using Maximal Information Coefficient (MIC), which is able to assess both linear and non-linear relationships between variables(33). Analysis was conducted in R 3.3.2 (R Core team) using the package Minerva(34). The analysis was bootstrapped to obtain confidence intervals and a p value for each correlation.

Using the year with the strongest correlation (birth year, see below) we set the density threshold and divided IRNP samples into 5 time periods, two periods of low density, two of high density

and one transition period (Figure 2.2, Table 2.1). The most recent time period (1997-2006) is anomalous due to fluctuating population densities following a 75% reduction in population size and includes moose born under densities ranging from 0.82-2.02 moose per km^2 with an average density of 1.86, just below our density threshold. We could not subdivide this time period and retain enough samples for meaningful statistical analyses, so we draw most of our conclusions from the first four time periods.

Dental Characters

Two observers (C. Rindali and C. Brown) independently surveyed 138 IRNP moose mandibles and CB surveyed 71 ONT mandibles for six features: signs of malocclusion, dental crowding, abnormal wear, tooth fracture, hypomineralization and dental enamel hypoplasia (DEH). All surveyed mandibles were radiographed in lateral view to look for LAGs and root abnormalities. Of the six features, only DEH were observed. DEH were categorized as pits, depressions, and linear enamel hypoplasias following the FDI DDE(35) (Figure 2.3). The frequencies at which individuals in each of our five periods exhibited DEH were compared using a chi-squared test in R. The hypoplasia occurrence data have an extreme left skew because post-weaning hypoplasias are rare. Consequently, to assess the differences between time periods we used relative risk assessment. Common in epidemiological studies (36–38), relative risk is used to assess the occurrence of relatively infrequent events and make pairwise frequency comparisons between groups, such as the moose in each of our six samples, those from each of the five IRNP time periods and the mainland.

Hypoplasia morphology varies with stress severity(39). Witzel et al. 2006 described the duration of the stress, the number of ameloblast (enamel secreting) cells affected, and changes in cellular morphology for common DEH manifestations (e.g. depressions, linear hypoplasiaas and large pits). We used their descriptions to assign a severity score ranging from 1-3 to assess relative levels of stress between moose which exhibited DEH (Figure 2.3). All teeth in an individual tooth row were scored. The FDI DDE Index used to assess hypoplasia morphology assigns a distinct number to each hypoplasia morphology, but the numbers do not increase with the stress necessary to produce each defect(40).

Mandible and metatarsus length

Mandible length was measured as the distance from the most ventral point of the mandibular notch (Figure 2.4) to the most caudal point of the mandibular foramen, permitting measurements on specimens with carnivore damage at the angle of the mandible. ONT mandible length data were captured by CB using digital photographs and ImageJ (http://imagej.nih.gov/ij/). IRNP adult mandibles less than 250mm (n=3) were considered outliers and excluded to facilitate meaningful statistical analysis (median adult length is 347.22 mm; median older adult length is 357.45mm).

Several factors can confound an assessment of the impact of population density on morphology, such as climate(14) and moose sex and age(41). The latter two can be expected to interact, as adult male moose continue to grow for several years past sexual maturity while females do not. We analyzed bone lengths as pooled samples as well as subdivided into prime-age (<9 years) and old-age (9+ years) moose to avoid the confounding effect of age on prime-aged male moose.

Because our length data do not follow assumptions of normality (mandible length, Shapiro-Wilkes W=0.79, p<2.2e-16, metatarsus length W = 0.89, p-value = 9.86e-07), we used a bootstrap in all analyses and chose tests robust to such data. To assess the effect of population density on moose mandible length between sexes and age groups we used a three-way ANOVA. To further analyze significant interactions between pairs of terms, such as sex and population density, we used two-way ANOVAs. For climate, we used the North Atlantic Oscillation (NAO) index, an established climate proxy for Isle Royale, and tested for correlations between the NAO and bone lengths, hypoplasia counts and population density using the Maximal Information Coefficient (MIC). ONT specimens were not included in two- or three-way mandible analyses because many lacked sex data and were aged using tooth wear rather than cementum annuli, and the former has a greater margin for error(42). However, we compared the Ontario to the contemporaneous moose from IRNP period 1 using a bootstrapped two-group comparison.

All code used in these analyses is available by request to the author. IRNP mandible and metatarsus length data are property of the Isle Royale Wolf Project. The exact values obtained through bootstrapped analyses will vary insignificantly from those presented here.

RESULTS

Density Threshold

The correlations between mandible length and population density of the birth year, gestation year and two years prior to birth were all weak and relatively noisy. For mandible length, the density of the birth year produced the only significant MIC value (birth year MIC 0.134, p=0.002) and the correlation between hypoplasia counts and population density was greatest for birth year (MIC 0.198, p=0.017), although the density of two years prior to birth was also significant (MIC 0.157, p=0.009). MIC scores range from 0 (statistically independent) to 1 (no noise). For simplicity, we used the population density of an individual's birth year to place them into groups of individuals that developed under high or low density conditions. Our results showed a significant effect on mandible length, metatarsus length and the mean number of DEH per hemimandible.

The effect of population size on teeth and stature

When all ages and sexes are pooled, IRNP moose born during the two high density periods exhibited significantly shorter mandibles (effect size = 4.89 mm, 95% CI [5.631, 10.418], p<0.0002) and metatarsals (effect size -6.097 mm, 95% CI [-5.943, 5.667], p<2e^{-16}) along with elevated frequencies of dental anomalies (DEH), relative to moose born during the two low density periods (Table 2.1, Figure 2.5). This suggests that overpopulation on IRNP had a negative impact on growth of teeth and bones. This is further supported by the comparison of mainland and IRNP moose. The frequency of DEH in IRNP moose ranges from 33% (period 1) to 81% (period 2) with a mean of 62.45% as opposed to 36% in the mainland moose sample. After period 1, the frequency of DEH in IRNP moose was 40%-200% greater than that observed in the ONT sample. Although metatarsal length data was not available for the mainland sample,

mandible length data indicates that the population residing on IRNP in period 1 had significantly

shorter mandibles than the contemporaneous mainland moose (effect size= 20.53mm, 95% CI

[7.1155, -10.51], p=1e-04). However, the sample size of measurable Ontario mandibles is small

(n=36) and the sex ratio of the IRNP period 1 sample is skewed toward females (1.68:1) which

may accentuate the size difference. Mandible length of IRNP moose varied only slightly over

first three time periods, and then declined sharply in period 4, the second of the high density

periods. Metatarsal length also shows its steepest decline between periods 3 and 4.

Individuals with shorter bone lengths tended to have more developmental enamel hypoplasias,

which were not evenly distributed across teeth and cusps (X^2=18.52, df=5, n=209, p<.001)

(Figure 2.6). The premolar teeth are nearly free of hypoplasias whereas certain molar teeth, such

as the m1 and m2, are particularly prone to them. Of all moose exhibiting enamel defects, 36.8%

(77/209), developed a linear defect on the buccal surface of the m2 approximately 3 mm above

the cemento-enamel junction while 22.9% (48/209) developed a linear defect on the buccal

surface of m1. The number of post-weaning enamel hypoplasias per mandibular ramus was

negatively correlated with mandible length (MIC 0.299, [0.275, 0.506], p=0.017), but mandible

length and the total number of enamel hypoplasias were not (MIC 0.267, [0.267, 0.510],

p=0.119) implying that a stressor other than post-weaning nutrition contributes to the total

hypoplasia count. Likely candidates are some aspect of life history, such as birth or weaning (see

Figure 2.2).

Dental enamel hypoplasias were recorded in all IRNP periods, but the frequency distribution is

significantly uneven over time (X^2=18.521, df=5, n=209, p<.001). DEH frequency peaks in

period 2, declines in period 3, and then rises slowly across periods 4 and 5. This pattern is driven

by male moose; the proportion of females with enamel hypoplasias did not change significantly

across periods (males X^2= 9.5065, df = 4, n=45; p-value = 0.04961; females X^2= 4.9811, df = 4,

n=33, p-value = 0.2892). When these data are broken down by time period and locality, the

relative risk of forming a defect, particularly while foraging independently of mother's milk, is

elevated in both high-density periods relative to low-density IRNP periods and the ONT sample

(Table 2.3, Figure 2.9a-b). Furthermore, the relative risk of forming a hypoplasia is elevated in

low density IRNP periods relative to lower-density ONT moose. IRNP moose from high-density

period 2 had the greatest risk of forming DEH, particularly post-weaning hypoplasias that can be

directly linked to insufficient forage. However, the risk of pit and missing enamel DEH

morphologies was not significantly elevated in any period (Figure 2.9c), demonstrating that

while the presence of DEH is associated with population density, the morphology is not.

Effect of age and sex of mandible and metatarsal lengths

 Age, sex, population density, and the interaction between sex and population density all had a

significant effect on the length of the mandible (Table 2.2). Pairwise investigation of sex,

population density and bone length showed that high population density had a significant effect

on median male mandible length (effect size= -5.28mm, 95% CI [-3.08, -9.33], p<0.001) but not

median female mandible length (effect size =-0.55mm, 96%CI [-1.82, 2.31], p=0.59). As

expected for a dimorphic species, male moose mandibles are always significantly longer (Figure

2.7), however the size difference is halved under high-density conditions (median effect size at

low density= 10.29mm; high density=5.33mm). Similarly, moose sex, population density and the

interaction between sex and density were significant contributors to adult metatarsus length.

Two-way analysis of metatarsus length, sex and density showed that population density but not sex had a significant association with MT length on its own. The fact that sex alone was not significant is surprising given the size difference between males and females (Table 2.2, Figure 2.8) (mean difference 6.157cm, [-4.84, 16.521] p=0.5118). Although final metatarsus length is strongly influenced by *in utero* nutrition(43), adult metatarsus lengths were not significantly shorter in individuals with greater numbers of total hypoplasias or hypoplasias incurred prior to weaning.

Other dental anomalies

Other signs of stress and malnutrition, specifically LAGs, malocclusion, dental crowding, abnormal wear, tooth fracture and hypomineralized enamel surfaces were not present in either moose population.

Impact of climate

Climate, as estimated by the NAO, was not strongly correlated with mandible length, metatarsus, total DEH or post-weaning DEH (Figure 2.10). While some MIC values were significant, the scatter of points is very large and the relationship detected by the MIC is both noisy and unclear when plotted.

DISCUSSION

Our analyses confirm that a moose density threshold exists on IRNP above which there is a significant decrease in mandible and metatarsus length and a concomitant increase in enamel hypoplasias. Density-dependent decreases in moose carcass weight and presumably skeletal size have been previously demonstrated(6,44), but here we show that signals of overpopulation may be preserved in skeletal measures alone, raising the possibility of estimating relative population size from changes in bone length. The frequency of post-weaning enamel defects appears to reflect food-limitation. When sexes are pooled for the IRNP moose populations, the relative risk of post-weaning enamel defects is significantly higher in high-density periods owing to the near-absence of post-weaning hypoplasias in both the low density period 1 and mainland Ontario moose. Nevertheless, period 1 Isle Royale moose had 1.18 times the chance of incurring a hypoplasia and 2.98 times the chance of incurring a post-weaning hypoplasia relative to their contemporaries on the mainland, suggesting that even the lowest population densities on Isle Royale can lead to resource limitation.

Dental enamel hypoplasias (DEH) differed significantly in frequency between the sexes and population density regimes, with density-related changes driven almost entirely by the effect on males. While Davis et. al (2013) found no difference in DEH frequency between the sexes in deer (*Odocoileus virginianus*), we found that male IRNP moose had significantly elevated frequencies of DEH during high density periods relative to low density periods. By contrast, female DEH frequency in IRNP moose was constant over time. Thus dental growth in male moose appears to have been much more negatively affected by food limitation than female moose. Moose generation time is short(45–47) and male reproductive success is driven by body size(48). Consequently, male ungulates seem more affected by conditions early in life than

females, due to the tendency for males to grow faster and for a longer period of time(44,48,49). In moose it seems that the sexes differ in their sensitivity to metabolic stress as early as birth, the time at which our earliest-developing character, the first permanent molar, develops.

Across all five IRNP time periods and both the island and mainland populations, enamel hypoplasias appeared in similar locations on 22.7% of first molars and 36.5% of the second molars. Using radiographs of developing moose mandibles, we determined that these defects were probably caused by birth (m1) and weaning (m2) as the enamel of the crowns is being secreted during these events (Figures 2.1, 2.11). During high-density periods, there was a significantly increased risk of developing an enamel hypoplasia on tooth crowns formed both prior to and during weaning (Figure 2.9a-b, Table 2.3). Like Wu et al. (2013) who studied caribou, we found a positive correlation between the frequency of weaning enamel defects and increasing population density. This suggests that DEH can be caused by weaning alone but are more likely to occur when food is limited.

The hypoplasia frequencies observed on Isle Royale (81%) are among the highest reported in wild populations of ungulates. While a declining population of Alaskan moose exhibited higher levels of enamel defects (93%)(50), the defects were not localized lesions like the DEH described here, but rather structural failures affecting most of the crown that may be linked to local geochemistry(51,52). Given that IRNP moose do exhibit reduced heterozygosity(53), it is possible but unlikely that the extremely high frequencies of DEH in IRNP moose area result of inbreeding. To date, DEH frequency has not been shown to increase in inbred populations; furthermore known genetic enamel disorders such as X-linked hypophosphatemia and

amelogenesis imperfecta are characterized by thinning and pitting of all enamel surfaces, abnormal tooth shape and malocclusion in human(23,54) and mouse models(55–57). None of these deformities were not observed in our IRNP moose samples. DEH in IRNP moose appeared on otherwise normal teeth with no signs of abnormal wear due to malocclusion or other factors. Moreover the majority of DEH in both the IRNP and ONT populations were located in constrained locations on the teeth and formed concurrently with birth and weaning. Similarly, the widespread pitting, abnormal wear and characteristic chalky appearance of enamel affected by hyperflourosis(23,58), another condition that causes enamel pitting in ungulates(59–61) was absent.

Unlike teeth that complete their growth within a year or two at most, bones continue to grow for several years after birth. In ungulates, adult metatarsus length is strongly influenced by the nutritional state of the calf's mother during gestation[41], but the growth trajectory is also influenced by conditions soon after birth. Similarly, mandibles continue to grow throughout the first four years of life(62) and therefore have the potential to capture the effects of food limitation over a longer period of time than teeth. Moose mandible and metatarsus lengths varied with population density as expected from existing life-history data; higher population density reduces food availability and moose stature. However, there is an interesting interaction between sex and population density. Like previous studies of other moose populations(63,64), we found that high population density has a much greater negative effect on male than female size. The greater effect of population density on males may be attributed to their longer period of growth, following a general trend of greater male investment in skeletal growth(16,41,48). Sexual selection in polygynous ungulates favors large male body size and delayed maturation while

55

female success increases with early sexual maturity and improved body condition rather than size(49,65). When calorie-limited, male skeletal growth slows while females may instead compensate through delayed breeding(13,64,66–68). Studying exclusively females, Ferguson et. al (2000) documented shortened mandible lengths in Canadian moose from medium and high-density populations during the growth period, though final adult mandible sizes did not differ. We were able to quantify mandible lengths in both sexes and found that while adult female moose mandibles were not significantly different, male moose mandibles remained shorter when the individual was born during high-density times.

Period 1 IRNP moose also had significantly shorter mandibles than contemporaneous mainland moose and this might have been due to the larger proportion of females in our IRNP period 1 sample. However, size reduction at this time is consistent with previous studies of metatarsal length(4,5) that found evidence for rapid dwarfing of the moose population in the century after their arrival on Isle Royale, a condition also suggested to be evidence of resource limitation and relatively high population densities. Combined with the increased risk of hypoplasia in period 1 relative to the mainland, it appears that some Isle Royale individuals were nutritionally stressed even during that comparatively low-density time. Thus, assessments of nutrition stress using enamel surfaces and bone lengths are primarily a means of gauging population density relative to food availability, rather than absolute levels of population density.

Mandible and metatarsus length tracked population density more close than did DEH frequency (Figures 2.2, 2.5). Within high density periods, the maximum population density is matched by minimum average bone lengths. Enamel hypoplasias, however, do not increase with population

density above the high-density threshold. Unexpectedly, IRNP moose born during the extreme population densities of period 4 did not have the highest frequency of enamel defects, even though moose from this period had the greatest reduction in metatarsus and mandible length. Moose from period 2, which encompasses a much lower population peak, had the most frequent DEH and the greatest risk of incurring a severe hypoplasia. The increased risk of incurring DEH caused by severe and longer-duration physiological stress indicates that conditions in the first months of life were more taxing in period 2. The apparent discrepancy between bone lengths and DEH may be due to another stressor that was present such as parasites or locomotor difficulties due to a dense winter snow crust, an added energetic expense not captured by the NAO index. It is also possible that plant biomass recovered more quickly in period 2 than during the historic population levels of period 4, and conditions improved during the extended growth period of the bones. While mandibles and metapodials tracked relative population changes at high density more closely than DEH, the lengths of these elements are significantly affected by age and sex. Given that individual age and sex data may not be obtainable for many collections, skeletal measures should be considered in conjunction with dental development particularly in the context of prehistorical applications.

Another complicating factor in using bone length as an indicator of nutritional stress is the possibility of compensatory growth later in life. For example, because mandibles continue to grow for several years after birth, a reduction in growth in earlier years might be reversed in later years if food is plentiful. Although one study found that moose do not show compensatory growth for poor conditions early in life(63), cervids and other ungulate species have been observed to do so(69–72) and thus compensatory growth in these species could obscure the

57

signal of population density. This is not true for teeth which complete their growth prior to age two and consequently, tooth enamel and DEH frequency can provide a better record of metabolic stresses that occur early in life than either mandible or metatarsal lengths.

Given that we conducted this study with an eye toward surveying ungulate populations throughout the historical and paleontological record, the preservation of characters is as important a consideration as how well they record of episodic stress. Because teeth preserve well and are common in the fossil record, dental hypoplasia frequency, particularly post-weaning, is probably a better record of historical overpopulation than mandible or metatarsal length. Long bones and mandibles are often incomplete or damaged, making it difficult to estimate total length, and sexual dimorphism in bone lengths can confound comparisons.

We stress again that the measures presented here provide only relative estimates of population density that should be combined with other climate and osteological data, for example estimates of nutritional stress in other taxa, to refine the estimate. In future work, we will assess the impact of life history on susceptibility to DEH using three cervid species. Additionally, malnutrition can be expected to affect all of the tooth tissues. In chapter three, we assess the growth of dentin over the population density regimes described here to compare the sensitivity of two tooth tissues that will be always preserved together in the fossil record. Together, these techniques will allow better characterization of ecosystems, particularly those represented by taphonomically unusual sites, for example those skewed by carnivore activity or tar seeps.

TABLES AND FIGURES

Table 2.1 Time periods of study, population density, frequency of dental enamel hypoplasias, average score of hypoplasias and mean bone length measures for two moose localities. Sample sizes are indicated in parentheses. IRNP= Isle Royale national Park; ONT= closest mainland Ontario moose.

Study Period	Years	Density Range (moose/ km^2)	Frequency of Moose Exhibiting DEH	Frequency Exhibiting Post-Weaning DEH	Mean DEH per Hemimandible	Mean Mandible Length (mm)	Mean Metatarsus Length (mm)
IRNP 1	(1959 - 1968)	1.05- 1.91	33% (21)	9.5%	1.54	357.5±12.69	388±9.13
IRNP 2	(1969 - 1974)	1.92- 2.33	80.95% (21)	42.86%	3.95	356.7±8.37	377.9±10.63
IRNP 3	(1977 - 1986)	1.41- 1.86	58.82% (34)	29.41%	1.87	361.7±8.91	385.72±11.2

IRNP 4	(1987 - 1996)	1.92- 4.04	65.21% (23)	34.78%	2.19	347.8±17.3	364±25.48
IRNP 5*	(1997 - 2003)	1.63- 2.05	74.28% (35)	29.62%	2.24	NA	373.92±16.3
ONT	(1950 - 1970)	0.16- 0.80	36% (71)	4.41%	1.02	374.07±19.1	NA

Table 2.2 Bootstrapped ANOVA Results. A single asterisk (*) indicated p<0.05 while a double a
sterisk (**) indicates p<0.01.

Variable	F Statistic Mandible	F Statistic Metatarsus
A) 3-Way ANOVA		
Sex	0.0448**	0.1332
Age	0.0525**	0.0021
Density (hi or lo)	0.0182**	0.1466**
Sex:Age	0.0028	0.0021
Sex:Density	0.0009*	0.0017
Age:Density	0.0053	0.2284*
Age:Sex:Density	0.4454**	1.2255*
B) 2-Way ANOVA		
Sex	0.0418**	0.0006
Density (hi vs lo)	0.0170**	0.1173*
Sex:Density	0.0008	0.0012

Table 2.3 Relative risk assessment of incurring one or more dental enamel hypoplasias (DEH) on all teeth and teeth formed after weaning across time and localities. The relative risk of pit and missing enamel DEH measures the occurrence of more severe and longer-lasting stress than the relative risk of all DEH types. IRNP= Isle Royale national Park; ONT= closest mainland Ontario moose.

Period	vs Period	X times the risk of 1+ DEH (all morphologies)	X times the risk of 1+ post-weaning DEH (all morphologies)	X times the risk of pit or missing enamel morphology
1	2	.5797	.281	.3846
1	3	.7173	.425	.5026
1	4	.6521	.359	.5952
1	5	.6366	.609	.7936
1	ONT	1.187	2.958	1.3
2	3	1.237	1.511	1.307
2	4	1.125	1.277	1.547
2	5	1.098	2.166	2.063
2	ONT	2.048	10.518	3.381
3	4	.909	.8455	1.184
3	5	.887	1.434	1.579
3	ONT	1.65	6.96	2.587
4	5	.976	1.69	1.333
4	ONT	1.820	8.23	2.184
5	ONT	1.864	4.854	1.368

Figure 2.1. Timeline of moose skeletal growth, tooth crown development, and metabolically significant life history events. Differences in male and female moose development that contribute to size differences are indicated as life history events. Data was compiled from radiographs, Isle Royale Annual Reports (isleroyalewolf.org) and radiographs and descriptions from Peterson (1950) and Peterson (1977).
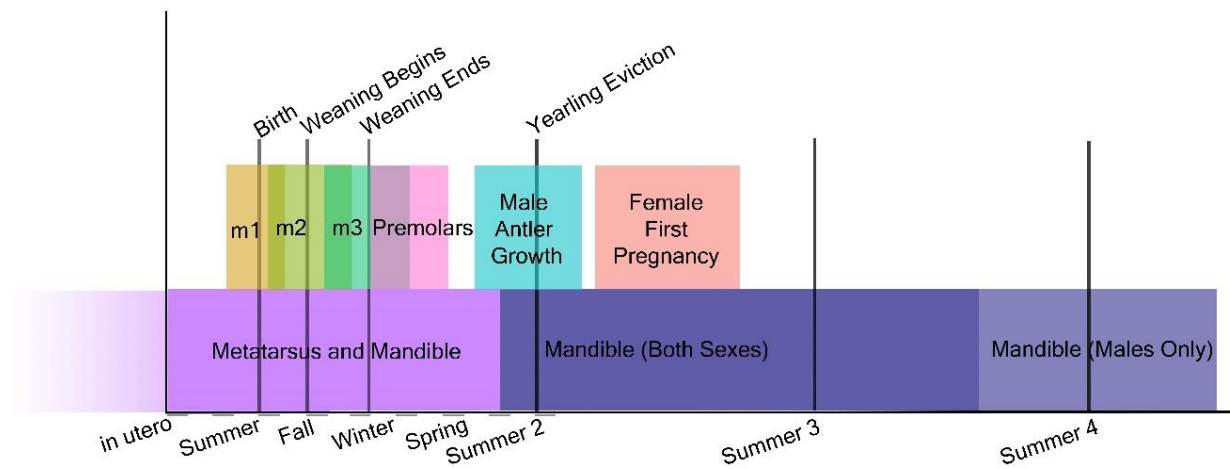
Figure 2.2. Moose population density over time. Sampled periods of high density are indicated by shading, as determined using the density threshold 1.92 moose per km^2 (red line, see text for details). The two colored bars indicate the estimated minimum and maximum density of the Ontario (ONT) mainland sample of moose. Note that low density IRNP moose are always at higher density than observed for our mainland sample.
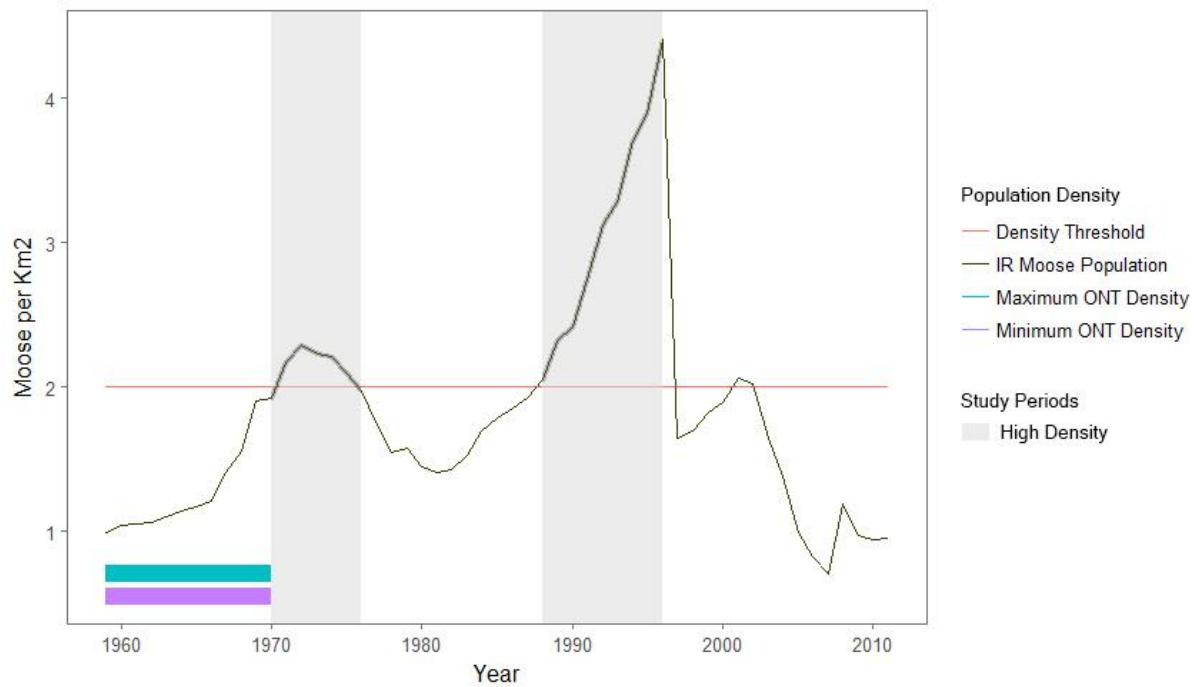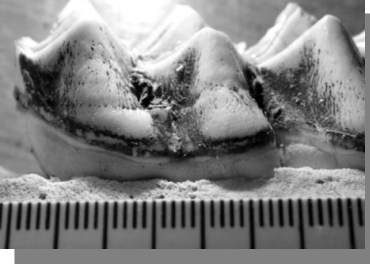
Figure 2.3. Isle Royale dental enamel hypoplasia (DEH) morphologies, their associated relative severity score, and a description of the ameloblast disruption that results in each morphology adapted from Witzel et al. 2006.

Hypoplastic Defect	Morphology	Score	Ameloblast Cohorts Affected
	Depression	1	Multiple; moderate impact and long duration
	Linear Enamel Hypoplasia (LEH), furrow morphology	2	Single; severe impact and very short duration
	Linear Enamel Hypoplasia (LEH), pit morphology	2	Single; severe impact and very short duration

	Pit	3	Multiple; severe impact and short duration
	Missing Enamel	3	Multiple; severe impact and short duration, Tome's secretory process lost

Figure 2.4. Anatomical landmarks used for mandible length measurements. The solid yellow

line represents measured jaw length. Image adapted from the Isle Royale Wolf Project.
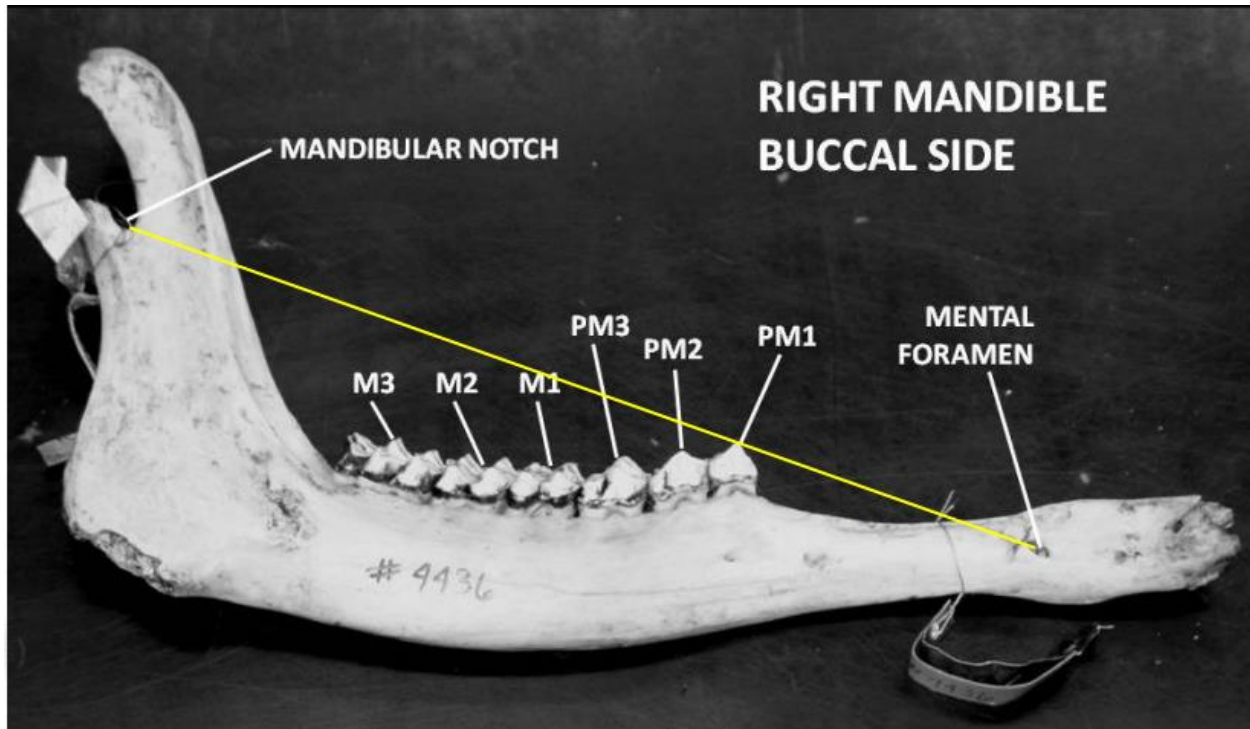
Figure 2.5. Trends in average metatarsus and mandible lengths and percent of individuals with DEH present per time period and locality. Note the inverse relationship between bone lengths (solid line) and DEH (dashed line). Data plotted here can be found in Table 2.1.

Average Bone Lengths and % DEH Over Time Periods
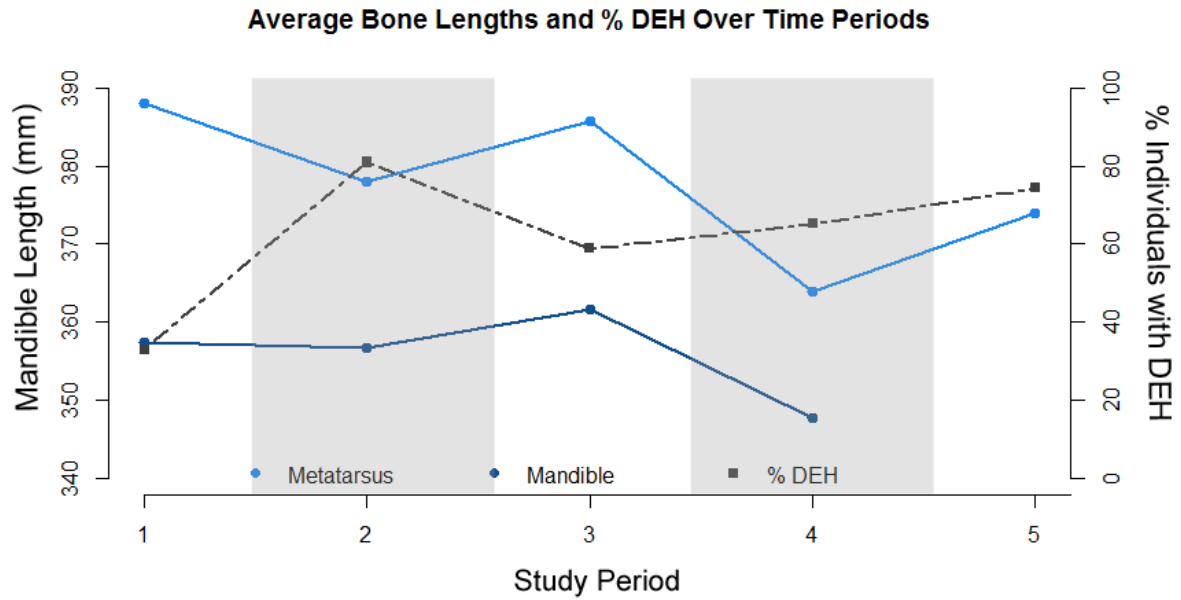
Figure 2.6. Proportion of moose exhibiting one or more hypoplasias per tooth and time period or locality. Teeth are displayed in approximate order of development and eruption. Grey and black bars indicate high-density periods.
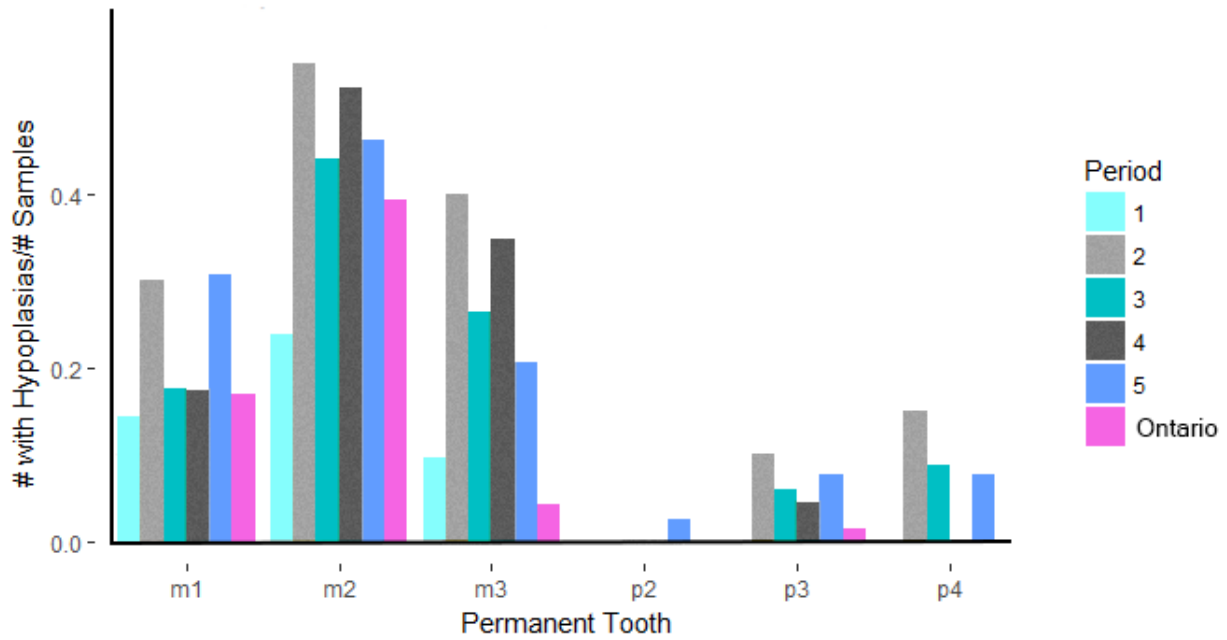
Figure 2.7. Boxplot of a) male and b) female mandible length by age and population density. Moose reach prime age (sexual maturity) before skeletal growth ceases.
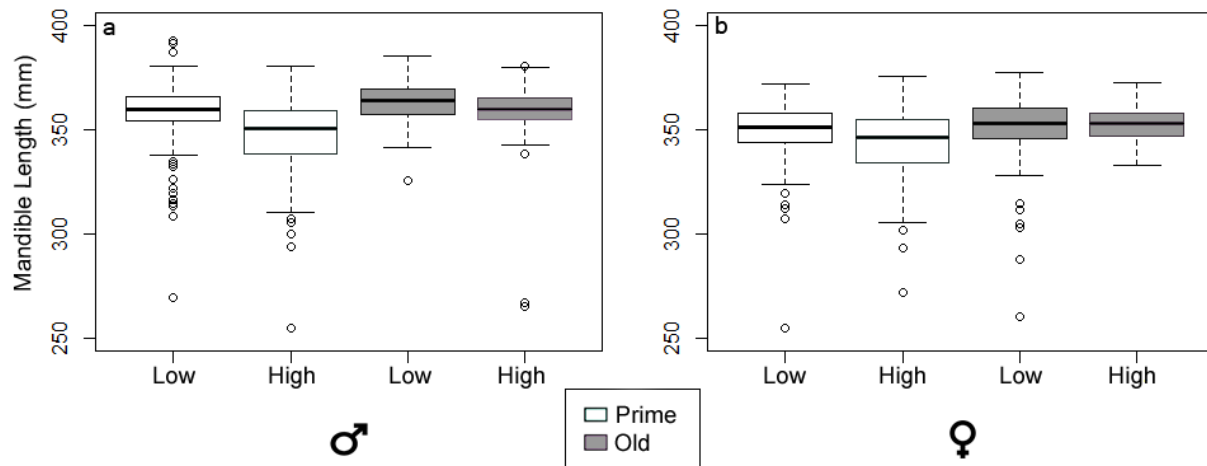
Figure 2.8. Isle Royale moose metatarsus length by population density and moose sex

Metatarsus Length
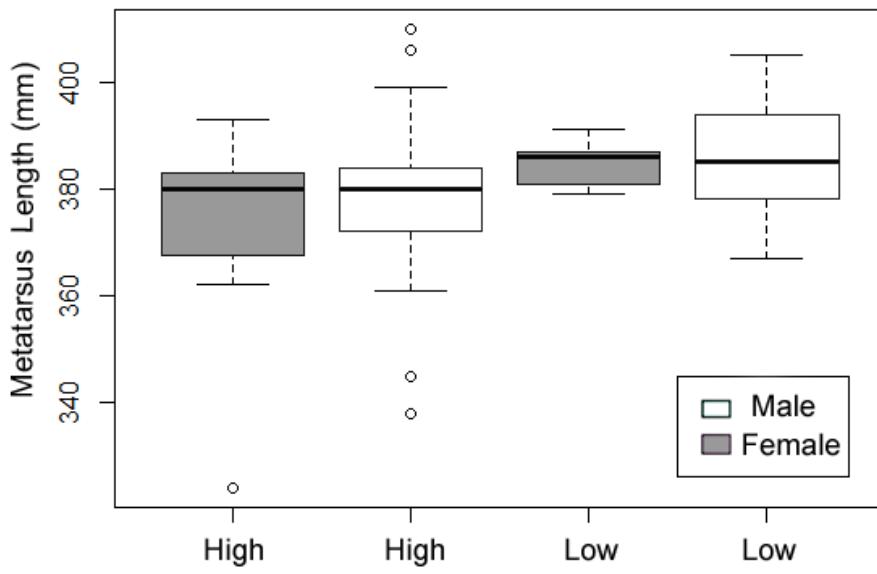
Figure 2.9. Heatmap depiction of the relative risk of hypoplasia types between periods. Colors represent the risk of hypoplasia in the period on the y axis relative to the corresponding period on the x axis. Data plotted here can be found in Table 2.3.
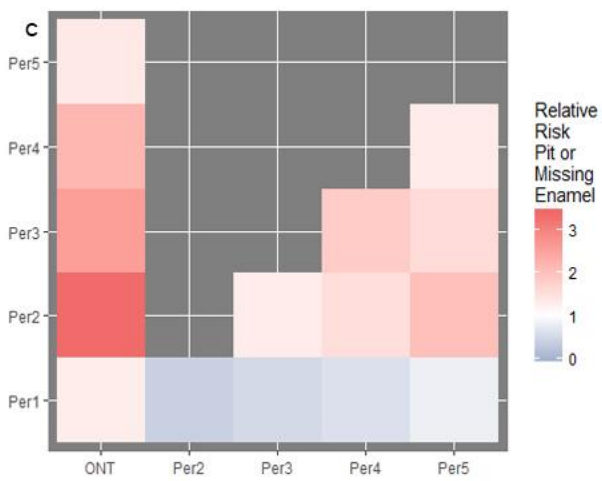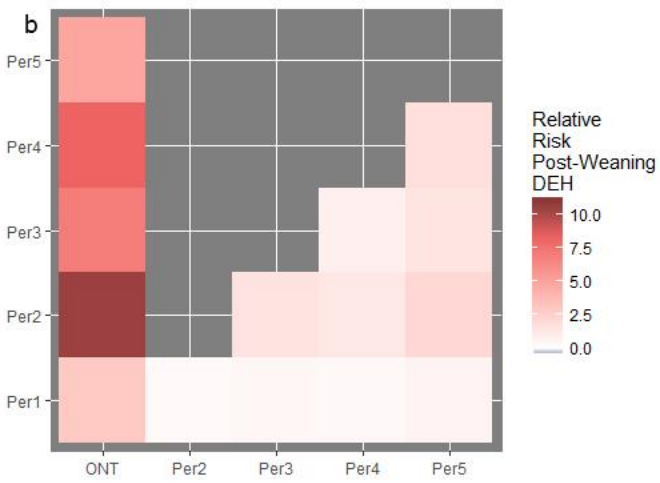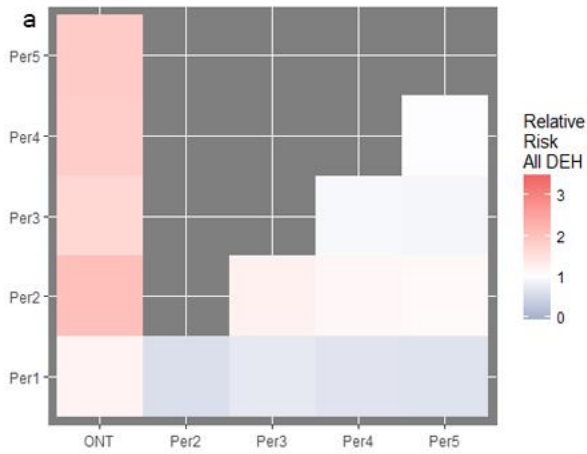
Figure 2.10. The relationship between the North Atlantic Oscillation (NAO), a proxy for winter severity, and surveyed skeletal and dental characters. A) NAO vs mandible length B) NAO vs total hypoplasia count C) NAO vs post-weaning hypoplasia count D) NAO vs metatarsus length.
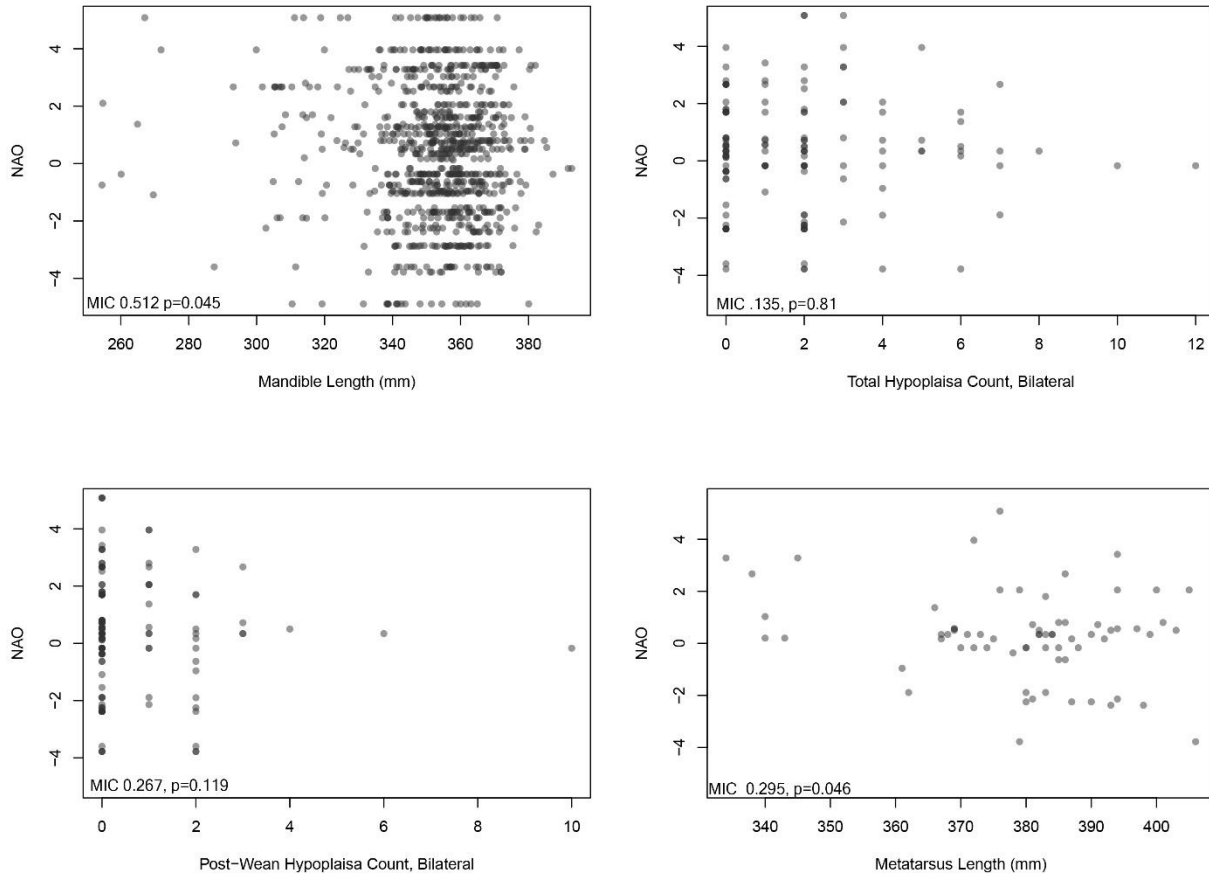
Figure 2.11. Radiograph images of moose tooth development from birth to full adult dentition. Moose are born while the M1 crown is mineralizing; weaning occurs between 5 and 6 months of age while the M2 crown is mineralizing and the M3 is beginning to form
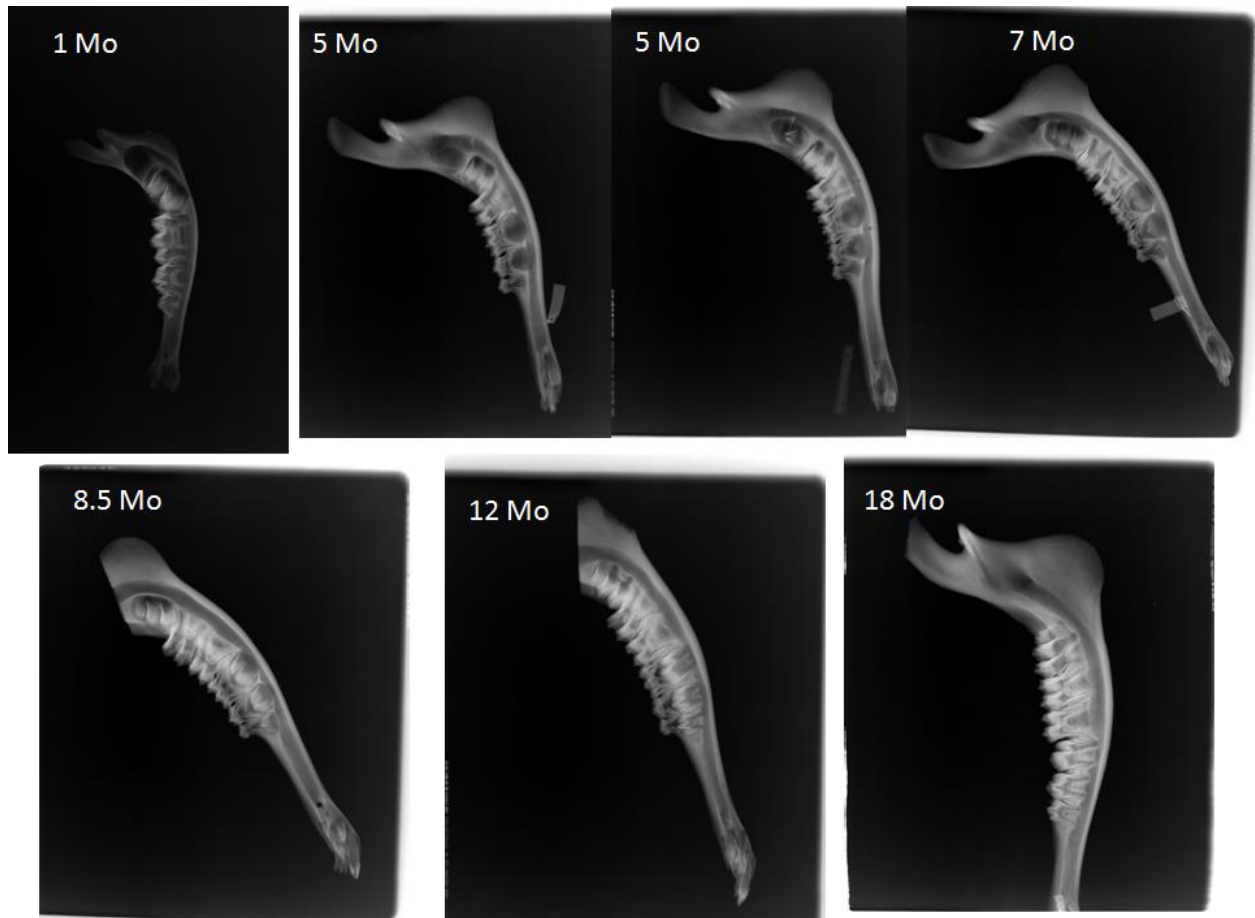
REFERENCES

1. Valkenburgh B Van, Hertel F. Tough Times at La Brea : Tooth Breakage in Large Carnivores of the Late Pleistocene Author (s): Blaire Van Valkenburgh and Fritz Hertel Published by : American Association for the Advancement of Science Stable URL : http://www.jstor.org/stable/2881931 J. 2017;261(5120):456–9.

2. Fisher DC. Season of death, growth rates, and life history of North American mammoths. In: West D, editor. Proceedings of the Internation Conference on Mammoth Site Studies Publication in Anthropology. University of Kansas; 2001. p. 122–35.

3. Ripple WJ, Beschta RL. Large predators limit herbivore densities in northern forest ecosystems. Eur J Wildl Res. 2012;58(4):233–47.

4. Peterson RO, Vucetich JA, Beyer D, Schrage M. Phenotypic Variation in Moose : the Island Rule and the Moose of Isle Royale. 2011;47(Lieberman 2009):125–33.

5. Silvia WJ, Peterson RO, Vucetich JA, Silvia WF, Silvia W. Variation in Metatarsal Morphology Among Subgroups of North American Moose (Alces alces). 1979;

6. Ferguson SH, Bisset AR, Messier F. The influences of density on growth and reproduction in moose Alces alces. Wildlife Biol. 2000;6:31–9.

7. Society W. Eruption Patterns of Selected Teeth in Three North American Moose Populations Author (s): Rolf O . Peterson , Charles C . Schwartz and Warren B . Ballard Published by : Wiley on behalf of the Wildlife Society Stable URL : http://www.jstor.org/stable/380. 2017;47(3):884–8.

8. Geist V. Deer of the World: Their Evolution, Behaviour, and Ecology. 1st ed. Stackpole Books; 1998. 421 p.

9. Peterson RO, John A, Drummer D, Spencer C. Ecology of arthritis. 2010;1124–8.

10. Hindelang M, Peterson RO, Hlndelang M. Osteoporotic Skull Lesions in Moose at Isle Royale National Park. 32(1):105–8.

11. Huot J. Review of methods for evaluating the physical condition of wild ungulates in northern environments. Québec Cent d'études Nord. 1988;50.

12. Peterson RO. of Wolves on Isle Royale by. 1996;

13. Society W. Growth in Domestic and Wild Reindeer in Norway Author (s): Eigil Reimers Source : The Journal of Wildlife Management , Vol . 36 , No . 2 (Apr ., 1972), pp . 612-619 Published by : Wiley on behalf of the Wildlife Society Stable URL :

http://www.jstor.o. 2017;36(2):612–9.

14.   Vucetich JA, Peterson RO. The influence of top-down , bottom-up and abiotic factors on the moose (Alces alces) population of Isle Royale. Society. 2010;271(1535):183–9.

15.   Article O. Linear Enamel Hypoplasia in Caribou (Rangifer tarandus groenlandicus): A Potential Tool to Assess Population Health. 2012;36(3):554–60.

16.   Peterson. North American Moose.

17.   Tonge H. Severe undernutrition in growing and adult animals. 1965;(14).

18.   Goodman AH, Rose JC. Assessment of Systemic Physiological Perturbations From Dental Enamel Hypoplasias and Associated Histological Structures. 1990;110:59–110.

19.   Guatelli-Steinberg D. What Can Developmental Defects of Enamel Reveal About Physiological Stress in Nonhuman Primates ? 1947;138–51.

20.   Dobney K, Ervynck A. Interpreting Developmental Stress in Archaeological Pigs : the Chronology of Linear Enamel Hypoplasia. 2000;597–607.

21.   Suckling G, Elliott DC, Thurley DC. The production of developmental defects of enamel in the incisor teeth of penned sheep resulting from induced parasitism. Arch Oral Biol. 1983;28(5):393–9.

22.   Goodman Rose DEH Indicators of Nutritional Status.pdf.

23.   Hillson S. Teeth. Cambridge Manuals in Archaeology. 1986. 376 p.

24.   Mead AJ, Mead AJ. Enamel hypoplasia in Miocene rhinoceroses (Teleoceras) from Nebraska : evidence of severe physiological stress. 2017;4634(April).

25.   Franz-Odendaal TA. Enamel hypoplasia provides insights into early systemic stress in wild and captive giraffes (Giraffa camelopardalis). 2004;197–206.

26.   Franz-Odendaal T, Chinsamy A, Lee-Thorp J. High prevalence of enamel hypoplasia in an early pliocene giraffid (Sivatherium hendeyi) from South Africa. J Vertebr Paleontol. 2004;24(1):235–44.

27.   Niven LB, Egeland CP, Todd LC. An inter-site comparison of enamel hypoplasia in bison : implications for paleoecology and modeling Late Plains Archaic subsistence. 2004;31:1783–94.

28.   Byerly RM. Palaeopathology in late Pleistocene and early Holocene Central Plains bison : dental enamel hypoplasia , fluoride toxicosis and the archaeological record. 2007;34.

29.   Witzel C, Kierdorf U, Dobney K, Ervynck A, Vanpoucke S, Kierdorf H. Reconstructing impairment of secretory ameloblast function in porcine teeth by analysis of morphological alterations in dental enamel. J Anat. 2006;209(1):93–110.

30.   Wilson MC. Bison Dentitions from the Henry Smith site, Montana: evidence for seasonality and paleoenvironments at an Avonlea bison kill. Davis LB, editor. Saskatoon: Saskatchewan Archaeological Society; 1988. 203-225 p.

31.   Davis HS. Enamel Hypoplasia as an Indicator of Nutritional Stress in Juvenile White-Tailed Deer. Georg J Sci. 2013;41(2):95.

32.   O'Connor T. The archaeology of animal bones. Am Anthropol [Internet]. 2000;104(1):206. Available from: http://eprints.whiterose.ac.uk/72766/

33.   Reshef DN, Reshef YA, Finucane HK, Grossman SR, Mcvean G, Turnbaugh PJ, et al. Detecting novel associations in large datasets. Science (80-). 2011;334(6062):1518–24.

34.   Albanese D, Filosi M, Visintainer R, Riccadonna S, Jurman G, Furlanello C. minerva and minepy : a C engine for the MINE suite and its R , Python and MATLAB wrappers. 2013;29(3):407–8.

35.   Federacion Dentarie Internacional. A review of the developmental defects índex (DDE Index). Int Dent J. 1982;42(6):411–26.

36.   Simon SD. Understanding the odds ratio and the relative risk. J Androl. 2001;22(4):533–6.

37.   McNutt L-A. Estimating the Relative Risk in Cohort Studies and Clinical Trials of Common Outcomes. Am J Epidemiol [Internet]. 2003;157(10):940–3. Available from: http://aje.oxfordjournals.org/content/157/10/940.full

38.   Zhang J, Yu KF. What's the Relative Risk?: A Method of Correcting the Odds Ratio in Cohort Studies of Common Outcomes\r10.1001/jama.280.19.1690. JAMA. 1998;280(19):1690–1.

39.   Witzel C, Kierdorf U, Dobney K, Ervynck A, Vanpoucke S, Kierdorf H. Reconstructing impairment of secretory ameloblast function in porcine teeth by analysis of morphological alterations in dental enamel. 2006;93–110.

40.   Clarkson J, O'Mullane D. A Modified DDE Index for Use in Epidemiological Studies of Enamel Defects. J Dent Res [Internet]. 1989;68(3):445–50. Available from: http://jdr.sagepub.com/cgi/doi/10.1177/00220345890680030201

41.   Society W. Relationship between Mandible Length and Carcass Weight of Moose in Norway Author (s): Bernt-Erik Sæther Source : The Journal of Wildlife Management , Vol . 47 , No . 4 (Oct ., 1983), pp . 1226-1229 Published by : Wiley on behalf of the Wildlife Socie. 2017;47(4):1226–9.

42.   Pérez-Barbería FJ. Evaluation of methods to age Scottish red deer : 2014;294:180–9.

43.   Palsson H. Effects of the plane of nutrition on growth and the development of the carcass quality in lambs Part I. The effects of High and Low planes of nutrition at different ages. J Agric Sci. 1952;42(1–2):1–92.

44.   Solberg EJ, Loison A, Gaillard J, Heim M. Lasting effects of conditions at birth on moose body mass. 2004;5(May):677–87.

45.   Geist V. On the behaviour of the North American moose (Alces alces andersoni Peterson 1950) in British Columbia. Behaviour. 1963;20(3):377–416.

46.   Van Ballenberghe V, Ballard WB. Limitation and regulation of moose populations: the role of predation. Can J Zool. 1994;72(Macnab 1985):2071–7.

47.   Gaillard J-M. Are moose only a large deer?: Some life history considerations. Alces. 2007;43:1–11.

48.   Garel M, Solberg EJ, S??ther BE, Herfindal I, H??gda KA. The length of growing season and adult sex ratio affect sexual size dimorphism in moose. Ecology. 2006;87(3):745–58.

49.   Kruuk L, Clutton-Brock TH, Rose KE, Guinness FE. Early determinants of lifetime reproductive success differ between the sexes in red deer. Proc R Soc B Biol Sci [Internet]. 1999;266(June):1655–61. Available from: http://www.ncbi.nlm.nih.gov/pmc/articles/PMC1690188/pdf/10501037.pdf

50.   Stimmelmayr R, Persons K. Incisor Tooth Breakage , Enamel Defects, and Peridontitis in a Declining Alaskan Moose Population. 2006;42.

51.   Clough MJ, MacKenzie CSK, Broders HG. The spatial variation of extreme tooth breakage in an herbivore and potential age structure effects. Ann Zool Fennici. 2010;47(4):261–71.

52.   MacKenzie CSK, Clough MJ, Broders HG, Tubrett M. Chemical and structural composition of Atlantic Canadian moose (Alces alces) incisors with patterns of high breakage. Sci Total Environ [Internet]. 2011;409(24):5483–92. Available from: http://dx.doi.org/10.1016/j.scitotenv.2011.08.066

53.   Wilson PJ, Grewal S, Rodgers A, Rempel R, Saquet J, Hristienko H, et al. Genetic variation and population structure of moose (Alces alces) at neutral and functional DNA loci. 2003;683:670–83.

54.   Wright JT, Johnson LB, Fine JD. Developmental defects of enamel in humans with hereditary epidermolysis bullosa. Arch Oral Biol. 1993;38(11):945–55.

55.   Gibson CW, Yuan ZA, Hall B, Longenecker G, Chen E, Thyagarajan T, et al.

Amelogenin-deficient Mice Display an Amelogenesis Imperfecta Phenotype. J Biol Chem. 2001;276(34):31871–5.

56.   Caterina JJ, Skobe Z, Shi J, Ding Y, Simmer JP, Birkedal-Hansen H, et al. Enamelysin (matrix metalloproteinase 20)-deficient mice display an amelogenesis imperfecta phenotype. J Biol Chem. 2002;277(51):49598–604.

57.   Poulter JA, Brookes SJ, Shore RC, Smith CEL, Abi farraj L, Kirkham J, et al. A missense mutation in ITGB6 causes pitted hypomineralized amelogenesis imperfecta. Hum Mol Genet. 2014;23(8):2189–97.

58.   Shupe JL, Christofferson P V., Olson AE, Allred ES, Hurst RL. Relationship of cheek tooth abrasion to fluoride-induced permanent incisor lesions in livestock. Am J Vet Res. 1987;48(10):1498–503.

59.   Kierdorf H, Kierdorf U, Richards A, Sedlacek F. Disturbed enamel formation in wild boars (Sus scrofa L.) from fluoride polluted areas in central Europe. Anat Rec. 2000;259(1):12–24.

60.   Kierdorf U, Kierdorf H, Fejerskov O. Fluoride-induced developmental changes in enamel and dentine of European roe deer (Capreolus capreolus L.) as a result of environmental pollution. Arch Oral Biol. 1993;38(12):1071–81.

61.   Kierdorf U, Kierdorf H, Sedlacek F, Fejerskov O. Structural changes in fluorosed dental enamel of red deer (Cervus elaphus L.) from a region with severe environmental pollution by fluorides. J Anat [Internet]. 1996;188 (Pt 1:183–95. Available from: http://www.pubmedcentral.nih.gov/articlerender.fcgi?artid=1167646&tool=pmcentrez&rendertype=abstract

62.   Alces M, Sand H, Cederlund G, Danell K. Geographical and Latitudinal Variation in Growth Patterns and Adult Body Size of Swedish Moose [Alces alces). Int Assoc Ecol. 2017;102(4):433–42.

63.   Solberg E, Garel M, Heim M, Grøtan V, Sæther B-E. Lack of compensatory body growth in a high performance moose Alces alces population. Oecologia [Internet]. 2008;158(3):485–98. Available from: http://dx.doi.org/10.1007/s00442-008-1158-z

64.   Garel Solberg Sæther Herfindal Høgda MEJB-EIK-A. The Length of Growing Season and Adult Sex Ratio Affect Sexual Size Dimorphism in Moose. Ecology. 2006;87(3):745–58.

65.   Clutton-Brock TH, Guinness FE, Albon SD. Red deer, behavior and ecology of two sexes. Vol. 10, Behavioural Processes. 1982. 440-441 p.

66.   Sand H. Life history patterns in female moose (Alces alces): the relationship between age, body size, fecundity and environmental conditions. Oecologia [Internet]. 1996;106(2):212–20. Available from: http://www.jstor.org/stable/4221250

67.   Keech MA, Bowyer TR, Ver Hoef JM, Boertje RD, Dale BW, Stephenson TR. Life-history Consequences of Maternal Condition in Alaskan Moose. J Wildl Manage [Internet]. 2000;64(2):450–62. Available from: http://www.jstor.org/stable/3803243

68.   Testa JW. Population dynamics and life history trade-offs of moose (Alces alces) in south-central Alaska. Ecology. 2004;85(5):1439–52.

69.   Watkins W. Compensatory growth of wapiti (Cervus elaphus) on aspen parkland ranges. Can J … [Internet]. 1991;69:1682–8. Available from: http://www.nrcresearchpress.com/doi/abs/10.1139/z91-233

70.   Wairimu S, Hudson RJ. Foraging dynamics of wapiti stags (Cervus elaphus) during compensatory growth. Appl Anim Behav Sci. 1993;36(1):65–79.

71.   Freetly HC, Ferrell CL, Jenkins TG. Timing of realimentation of mature cows that were feed-restricted during pregnancy influences calf birth weights and growth rates. J Anim Sci. 2000;78(11):2790–6.

72.   Luke DA, Tonge CH, Reid DJ. Effects of rehabilitation on the jaws and teeth of protein-deficient and calorie-deficient pigs. Cells Tissues Organs. 1981;110(4):299–305.

CHAPTER 3

Population Level Trends in Wild-Living Moose Dentine Growth Under Varying Levels of

Population Density

INTRODUCTION

The relative abundance of species in fossil assemblages is notoriously difficult to

determine due to biases in preservation such as those due to body mass or habitat preference.

However, teeth may offer a partial solution. Mammalian teeth fossilize exceptionally well and

contain a wealth of information on growth rate in a form that is easily interpreted. The primary

tooth tissues- enamel, cementum, dentine, and the mandibular bone that contains them, preserve

information about an animal's health and environment over daily, weekly, and yearly

increments. These tissues are sensitive to metabolic stress during their formation, and in the case

of dental tissue, yield an indelible record of an individual's health during development. In

particular, the formation of enamel and dentine can be inhibited by food limitation[1], a

condition that often characterizes high-density populations. While developmental defects of

enamel can result from a single, severe event such as birth or weaning, dentine provides a long

term, sensitive record of the individual's health. Like enamel hypoplasia, interrupted dentine

formation during the growth or mineralization phase leaves characteristic marks that persist after

death. Building upon Chapter 2, we investigate the effect of population density via food

shortages resulting from population irruptions in moose on Isle Royale. Irregularities in the

incremental growth of tooth tissue have been linked to variety of stressors but they have not been

conclusively linked to fluctuating population densities prior to this study of large, North

American ungulates (but see Fisher et. al 2001[2]).

Incremental growth occurs in mammal dentine as alternating dark–light couplets visible under regular and polarized light. Incremental growth structures have been used extensively for the determination of life history data and several studies have documented the effects of environmental and physiological events on the growth of dentine. Conditions such as age of maturation(3), seasonality(2–5) ,rates of ontogenetic development(6) , pregnancy and lactation(3,7,8), parturition(9),nutritional stress caused by El Niño(10), and hibernation events(11–13) have been shown to affect rates of dentine development and composition. Incremental markings form daily in dentine, and when visualized in sectioned teeth, are known as "von Ebner lines". The circadian periodicity of von Ebner lines in dentine (Fig. 3.1) has been demonstrated experimentally for a diversity of vertebrates including two ungulate species: pigs (*Sus scrofa*(14)) and sika deer (*Cervus nippon*(15)). Increment formation rates are comparable across ungulates occupying high-latitude and temperate regions(16), such as reindeer (*Rangifer tarandus*) and red deer (*Cervus elaphus*), thus we expect that von Ebner lines in moose dentine represent daily increments, though we could not experimentally label increments to confirm the periodicity of the measured features.

Incremental growth analysis examines tissues that, by nature of their regular deposition, are more easily linked to metabolic stress and is expected to correlate better with population density than dental enamel hypoplaisa (a presence-absence feature) or bone lengths (a sexually dimorphic trait). Like our assessment of macroscopic characters investigated in Chapter 2, this study differs from most previous incremental growth studies in that it utilizes large populations of wild animals for which nutritional status and environmental factors are known and aims to assess health throughout the population rather than for an individual. In most or all prior studies

84

of incremental growth, entire teeth were extracted, thin sectioned, and examined under a microscope. Because we wish to apply our methodology to fossil specimens where such destructive sampling is undesirable and often not possible, we developed a novel method that relies on a single molar tooth root, thus leaving the tooth crown intact. Selecting only a small and consistent region of the molar root of the last tooth to erupt for incremental study allowed us to study post-weaning nutrition in these individuals and while minimizing the destruction of specimens by avoiding the need to section the anterior tooth roots or crowns, which may be valuable for future studies by others.

Detailed knowledge of incremental growth patterns and developmental timing, in conjunction with data regarding population density and nutritional status of these ungulates, should make it possible to statistically evaluate the effects of nutrition and population size on average incremental growth rates of individuals within a population. While malnutrition has not been explicitly linked to decreased increment widths in wild animals, there is some experimental evididence that tooth crown and root size decrease after severe malnutrition[17], which indicates that dentine formation can be inhibited. Based on the negative responses of enamel formation and long bone growth to elevated population density in the same individuals studied here (Chapt. 2) and in the population as a whole[18,19], we expected to see a reduction in the width of incremental features as population density increases. These results will contribute to understanding how variations in environmental conditions affect dental incremental growth in mammals, and will be immediately applicable to the study of fossil teeth in our planned study of Pleistocene populations as well as archaeological samples.

METHODS

We took a series of radiographs of seven juvenile moose mandibles (Fig. 2.11) to fill in gaps in the mandible growth series presented in Peterson (1950)(20). We sampled tooth roots from moose for which we had assessed enamel condition and mandible length (see Chapter 2). The last developing root, the most caudal root of the lower third molar (m3) was extracted from 40 individuals split evenly between both sexes and 4 periods of high and low population density. To avoid confusion with our assessment of enamel defects and bone lengths relative to moose density, which used five time periods, dentine study periods are labeled as periods d1-d4. Periods d1 and d4 are low density while d2 and d3 are high (Fig. 3.6). Poor preservation or large regions of sclerotic dentine (e.g., Fig. 3.2a,d) obscured the majority of incremental features in five specimens, leaving us with a sample of 35 individuals, split nearly evenly between sexes and high and low density periods (Table 3.1).

We aimed to develop a protocol that accurately assesses the effects of population density and nutrition on tooth development while minimizing the effects of seasonality in our comparisons. To do so, we restricted the region of study to the last-formed tooth root to eliminate the possibility of including increments that were developing earlier, during the individual's fetal development or while the individual was obtaining nutrition from its mother's milk. The dentine increments studied must correspond to a period in the life history of an individual when it is not buffered from environmental stressors through reliance on maternal milk. Because root dentine is the last part of the tooth to develop and the growth record ceases when tooth development is completed, studying the roots of the molars should enable the largest sample size possible of post-weaning, independently foraging individuals. Second, restricting the region of study to a specific location within the tooth should minimize the effects of seasonality in the growth rate

data. Because most species of wild ungulates bear young once a year within a narrow window of time, the season of development of a specific region of a tooth can be resolved.

Our minimally destructive method entails a 31.75mm circular window cut in the mandibular cortical bone superficial to the root selected for study. The window allows access to the posterior m3 root, which is only partially attached to the neighboring taurodont roots. Roots were carefully dissected out of the cancellous bone using a Dremel tool fitted with a 545-diamond wheel approximately 4mm distal to the cemeto-enamel junction. Extracted roots were embedded in Osteo-Bed Plus Embedding Kit (methyl methacrylate resin), Polysciences, Inc. Embedded roots were thin-sectioned using a low-speed IsoMet saw and mounted on microscope slides using epoxy glue, lapped down and polished to 60-100 µm thicknesses using a HandiMet grinding apparatus. On average, six 1.5mm sections were cut from the root, of which the first (cervical), third (mid-root), and fifth (apical) complete sections were used. Bonding the specimen to a glass slide made it easier to prepare a uniformly thin section. To avoid expansion of tooth structure from water absorption and subsequent detachment from the slide, ethanol was used as the grinding medium.

Because of the flexibility and visualization tools afforded by the microscope, prepared sections were measured using a Leitz DialuxPol polarizing petrography microscope outfitted with a 4-axis universal stage. The slides were placed between quartz optical spheres with a refractive index of 1.516 with a thin layer of glycerin on each side, closely approximating the refractive index of dentine(21). The optical spheres allow for viewing of specimens from any angle thereby facilitating counts of increments in areas with poorly resolved incremental features. On each slice, two non-overlapping areas of 27-43 (average =33) well-preserved increments were quantified. Curved regions of the root were avoided because in the curved

portion the width of the root varies noticeably, leading to variation in the calculated rate (22).

The microscopic structure of the dentine was examined throughout the entire slice to identify the

presence of interglobular dentine or anomalies in incremental structure. Without an estimate of

periodicity, a daily growth rate could not be determined. Increment width was measured using a

reticle calibrated using a stage micrometer placed in the optical sphere.

Previous work has suggested that a density greater than two moose per km^2 (total island

population equal to 1,071) may result in stunted bone growth, particularly in the length of the

mandible(23). In addition, the carrying capacity of the island, as determined by browse

availability surveys made between 1945 and 1970, was estimated to be 1000 moose (or 1.83

moose/km^2). We used the average of these two density estimates (1.92) as the density threshold

beyond which moose are expected to show evidence of stress. Peterson and Maclaren(24)

linked the effects of malnutrition (resulting from inadequate forage) on moose population growth

(and therefore body condition) two years later . Malnutrition due to overpopulation could also

affect the individual through the condition of the mother in the gestation year, or when the calf is

foraging independently during its first winter after birth. To determine which year's population

density should be considered in our analyses, we first looked for correlations between the

population size of each candidate year and increment width. We explored the correlations

between population size and increment width using Maximal Information Coefficient (MIC),

which assesses both linear and non-linear relationships between variables(25). MIC values range

from 0 (random) to 1 (a perfect correlation). Analysis was conducted in R 3.3.2 (R Core team)

using the package Minerva(26). The analysis was bootstrapped to obtain confidence intervals

and a p value for each correlation.

To assess the effects of different density regimes, we used primary dentine increment width to infer growth rate. Each individual's average circadian growth rate was calculated for each of three histological cross-sections (cervical, mid-root, and apical; Figure 3.3) of the m3 root. An overall rate for each individual was calculated as an average of the values of the three cross-sections. The purpose of using three different cross-sections for each individual's root was to minimize the effects of error in selecting homologous locations on the m3 root among individuals. By consistently analyzing three different regions of the root, we hoped to eliminate, as much as possible, the effects of seasonality or variation in growth rate unrelated to nutritional status that might occur during the development of the root. We compared median difference between growth rates of low and high density groups using a bootstrapped two-group comparison. To look for correlation between increment width and population density and between width and our climate proxy, we used the Maximal Information Coefficient (MIC).

RESULTS

The median width of moose dentine circadian increments was 16.57 ± 1.46 µm. Based on radiographs and observations of juvenile specimens, we can see that the posterior m3 completes crown development by 8.5 months, followed by complete root extension by 14 months and primary growth of dentine is complete by 2 years of age (Table 3.2, Figure 3.4). With a median circadian increment width of 16.57µm and an average primary dentine width of 1.47mm the increments counted in our study probably formed between 14 and 20 months of age, and thus largely during an individual's second fall and early winter. The increment width appeared consistent between sections (Fig. 3.5) suggesting that there are not major fluctuations in appositional growth rates throughout root development. We did not see evidence of strong

89

seasonal differences in dentine growth, which is confirmed by the lack of significant correlation between the our climate proxy and increment width at any section of the root. The middle section of the m3 root has a lower median value and lower variance than in the other two sections, which suggests that the middle slice captures a period of slower increment formation, but not enough to significantly affect the median value. The middle slice also exhibits a tighter correlation between increment width and population density, which would be expected if the decrease in growth was due to seasonal food limitation exacerbated by overpopulation rather than seasonal changes in moose metabolism.

Dentine mineralization anomalies were present in all study periods. Bands of hypermineralized dentine were observed in the majority of specimens (Fig. 3.2a,b), while one individual with unusual granular dentine was present in each study period (Fig. 3.2c,e-f). Sclerotic dentine was present to some degree in most samples. Sclerotic dentine is a normal response to abrasion and irritation, and the amount of sclerotic dentine in the root increases with age(27,28). Consequently, we did not consider sclerotic dentine to be an anomaly.

Whereas the strongest association between population density and interrupted enamel growth (Chap. 2) was that of the birth/weaning year, this was not the case for incremental lines of growth. There was no significant difference between incremental growth width of moose born under high or low density conditions and the overlap in the variance is substantial (Figs. 3.7, 3.8). When viewed by period, the difference in median values is not significant but there appear to be opposing responses to high-density conditions in periods d2 and d4. Instead, the width of increment width was most closely correlated with the population size two years prior to birth/weaning. The correlation between increment width and the population size two years prior to birth/weaning was positive and nearly significant (MIC 0.39, 95% CI [0.29, 0.73], p<0.057)

(Fig. 3.6). Visual inspections of sex differences, a factor that had a significant effect on enamel and mandible growth (see Chapter 2), did not suggest that dentine apposition rates vary between the sexes.

DISCUSSION

The overall average circadian increment width we observed in moose dentine from Isle Royale was 16.57 ± 1.46 µm, well within the range of values observed in other vertebrates (11.25-19.25 µm(29)), and similar to that of sika deer (17.3µm(15)). Average increment width remained constant through time and between density regimes, in contrast to our predictions and in spite of the presence of effects on development of enamel and bone under these same conditions. In addition to the absence of significant correlation between population density and growth rate, mean growth rates were highest during peak high density in all root sections analyzed: the two low density periods have similar mean values (16.56 µm, 16.66 µm), high-density period d2 is slightly lower (15.92 µm), while period d3, the time of peak density, has the highest rate (17.01 µm). When both high-density groups and both low-density groups are combined, respectively, the trend toward greater incremental growth rates under high-density is clearer. The near-significant correlation between population size and dentin growth was unexpected given the greater frequency of dental enamel hypoplasias observed in these same individuals (see Chapter 2). It is interesting that bone and enamel development showed a strong response to metabolic stress, while dentine did not--a response which may be dictated by the structural role of the tooth root.

Moose teeth erupt into the oral cavity earlier than in the other cervid for which incremental growth lines have been measured, the sika deer. While sika deer teeth reach full

91

eruption at 26 months of age, moose erupt all of their permanent dentition by 14 months of age. Tooth roots support the tooth during chewing, and thus it may be advantageous to form roots as quickly as possible and bring the teeth into occlusion early in life(30). Resource availability in the early successional forests favored by moose is unpredictable and can negatively impact juvenile survival. Such uncertain conditions favor short generation times and early somatic maturity(31)(32). The full adult dentition erupts faster in moose than red deer, a species with similar reproductive maturation and smaller body size, indicating that early sexual maturity alone is not driving rapid moose tooth development. Given that resource availability has selected for accelerated maturity and rapid tooth eruption in moose, perhaps it is not surprising that the biological rhythm of dentine secretion was not interrupted by malnutrition because tooth roots are necessary for food processing. Malnutrition resulting from increased population density may affect bone length, but not dentine because teeth are prioritized over bone during development in ungulates. When Tonge and McCance (1965)(17) experimentally placed pigs on extreme low calorie diets, they found that dental growth was given developmental priority over the mandibular growth, leading to individuals with normal sized teeth situated in jaws too small to accommodate them. A less extreme version of this mechanism may explain the fact that dentine growth in moose is not slowed under high-density conditions while mandible growth is truncated (Chapter 2).

Unlike what we observed for both enamel defects and bone lengths, there were no apparent differences between males and females in the incremental growth of dentine. Why should the two dental tissues respond differently? It is difficult to understand the incongruous responses of bone, enamel and dentine under the high-density conditions of periods d2 and d3. Although both periods d2 and d3 were classified as high density, the population density of period

92

d2 moose was much lower than that of period d3. Nevertheless, period d2 moose were characterized by the highest frequency of enamel hypoplasias and only a slight reduction in dentine apposition (at the middle slice). By contrast, the more populous period d3 moose had fewer enamel hypoplasias, but the shortest metatarsi and mandibles, alongside the highest rate of dentine growth for any time period. This suggests that the factors that affect both DEH frequency and bone length are different from those that affect dentine apposition rates.

Although our sample of Isle Royale individuals is large enough to refute the notion that high population density decreases the rate of dentine apposition, it also reveals substantial variation among individuals born under similar conditions. Because we sampled wild individuals, variation in factors such as the quality of maternal care or access to Isle Royale's unevenly distributed winter browse(33) could have a profound impact on individual growth. More thorough sampling of the population may reveal a clearer relationship between the effects of overpopulation and the skeletal health of the population as a whole. Nonetheless, the unexpectedly high dentine growth rates observed in extreme high density period d3 moose may not be due to small sample size, but rather a response to prior nutritional stress, as evidenced by the very high frequency of enamel hypoplasias on the earlier erupting m1 and m2 of period d3 moose.

A possible acceleration of dentine growth after food limitation is not without a biological basis. Compensatory growth or catch-up growth is a phenomenon observed in a variety of animals in which they grow at an accelerated rate following caloric restriction(34). This mechanism may allow individuals to reduce their nutritional requirements when food is scarce and catch up to a normal growth trajectory when conditions improve, thereby increasing the chance of survival to maturity(35). Compensatory growth has been observed as increases in body

mass and bone lengths in a variety of ungulates under experimental conditions: reindeer (*Rangifer tarandus*(36)), elk (*Cervus canadensis*(37)), domesticated pigs (*Sus scrofa*(38)) as well as in wild populations (*Ovis canadensis*(39); *Cervus elaphus*(40,41) ; *Odocoileus virginianus*(42)). Despite observations in other cervids, there have been no confirmed cases of compensatory growth in moose. Keech et al. (1999)(43) found no evidence for compensatory growth in body mass in juvenile Alaskan moose, but their study included only ten female moose. Likewise Sohlberg et. al (2008)(44) found no evidence for compensatory growth in mass in a study of 101 moose born under densities of <0.5 moose/km^2. These studies used carcass weight and bone length to assess growth, but our work suggests that dentine responds differently to nutritional stress than bone, and this likely relates to differences in how teeth and bone are prioritized.

Food limitation disrupted the mineralization of dentin in the Isle Royale moose in both high and low-density periods. Dentinogenesis occurs in two stages that occur in rapid succession. First, a collagenous predentine is secreted and globules of crystalline calcium hydroxyapatite form, followed by a secondary mineralization phase that coalesces the crystals in a regular, layered form(45). In parts of the root where the secondary phase of mineralization fails to occur, less mineralized dentine forms between the globules, forming interglobular dentine. Thus, while enamel mineralization only occurs when the full tissue thickness is completed, dentine is simultaneously growing by apposition and mineralizing in nearby increments. The lack of clear temporal segregation could mean that both secretion and maturation would be affected by malnutrition in the same way, but that was not the case for the Isle Royale moose.

Unlike rates of incremental growth of dentine which were fairly constant in Isle Royale moose, the process of mineralization of the tissue was more variable during all study periods, as

evidenced by multiple-increment, concentric bands of hypermineralized dentine. Of our usable samples, 30 of 35 individuals had at least one such band in the root, typically in the middle of the cervical and mid-root sections (Fig. 3.2a,d). Areas of hypermineralized (sclerotic) dentine form progressively as individuals age, but they typically begin at the cemento-enamel junction, progress from apical to cervical and often exhibit a "butterfly" appearance in single roots (28). We observed the "butterfly" patterning in some moose, as well as obvious dead sclerotic tracts running perpendicular to the incremental features, but the appearance of the hypermineralized bands (alternating normally and hypermineralized bands) and location (more often in middle and cervical slices) are not consistent with the typical pattern. We observed banded hypermineralized dentin in individuals ranging in age from 3 to 15 years (young prime-aged and old moose), suggesting that it is not entirely a response to aging(46). The relatively consistent location may be evidence of seasonal changes in growth in the winter during the appositional growth and maturation of the interior of the root (Fig. 3.3.iii) or they may represent a normal progressive change in moose dentine with age. However, Kelvezal(22) recorded a similar banded appearance in female seals (*Phoca vitulina*) and dolphins of both sexes (*Tursiops truncatus*). They felt that the hypercalcified and sclerotic bands (which they called Strongly Contrasting Lines, or SCLs) were linked to breeding, but acknowledged that they appear in both sexes in the dophin and were interpreted by Manzanilla(10) as evidence of a stressful El Nino event. In addition to these transparent bands, dentine with a granular appearance was present in various locations in one specimen from each study period, indicating that there were additional, non-seasonal changes in dentine formation. These bands of granular dentine could represent changes in the growth rate of dentin, similar to what has been inferred for the granules near the cemento-enamel junction (i.e. the granular layer of Tomes)(45). Reduced bone length and enamel hypoplasia rates indicate that

even the lowest density periods on Isle Royale are more stressful than on the adjacent mainland (see Chapter 2). Investigation of a low-density, non-insular population might show that the heterogenous dentine seen in the Isle Royale population is uncommon in typical wild populations and could therefore provide a signal of overpopulation in both historical and fossil ungulate populations.

Overall, incremental growth of dentin in moose was not slowed by episodes of malnutrition, allowing to conclude that malnutrition does not have comparable effects on bone, enamel and dentine. Incremental growth studies typically assess a handful of individuals to capture trends in species life history or the health of individual animals. We looked at a much larger number of individuals in the hopes that we could capture population-level trends. What we found was substantial variation between individuals that allowed us to see shifts in dentine growth rates, but no significant associations between averaged incremental growth rate and climate or population size. Growth rates from individuals born under high-density conditions tended to be higher (Figure 3.8), suggesting a compensatory growth mechanism. The near-significant correlation between high population density and accelerated dentine growth in IRNP moose was the opposite of what we had predicted based on the growth of enamel and bone, indicating that dentine secretion may be given precedence during development over these other tissues. We can only speculate about the reason for this discrepancy, but certainly it is clear that dentine apposition under various levels of nutritional stress deserves further investigation both in this famous island population and in mainland moose populations.

TABLES AND FIGURES

Table 3.1. Tooth root sample size, sex distribution and population density range per density regime.

Sex	High 1.92-4.41 moose/km^2	Low 0.98-1.74 moose/km^2
♀ Female	8	9
♂ Male	9	9

Table 3.2. Approximate timeline of lower third molar development in Isle Royale moose (*Alces alces andersonii*).

Molar 3 timeline:	Illustration	Description	Season
5 months		Crypt visible	Fall, end of weaning period
7 months		Crown mineralizing, no root	Winter
8.5 months		Crown complete	nearly spring

9 months		Root beginning to extend	Spring
12 months		Root extension and mineralization in process, occlusion beginning	Summer
13-14 months	3.3.i	Root extension nearly complete, root is hollow	Summer prior to first pregnancy and rut
17months	3.3.ii	Root extension complete	Second fall
20 months	3.3.iii	Primary dentine filling in toward pulp cavity	Second winter
24 months	3.3.iv	Primary dentine growth complete	Summer

Figure 3.1. Circadian markings in the dentine of an axiobuccalingually sectioned moose molar root #4060 viewed under polarized light. Increments are marked with a series of arrowheads.
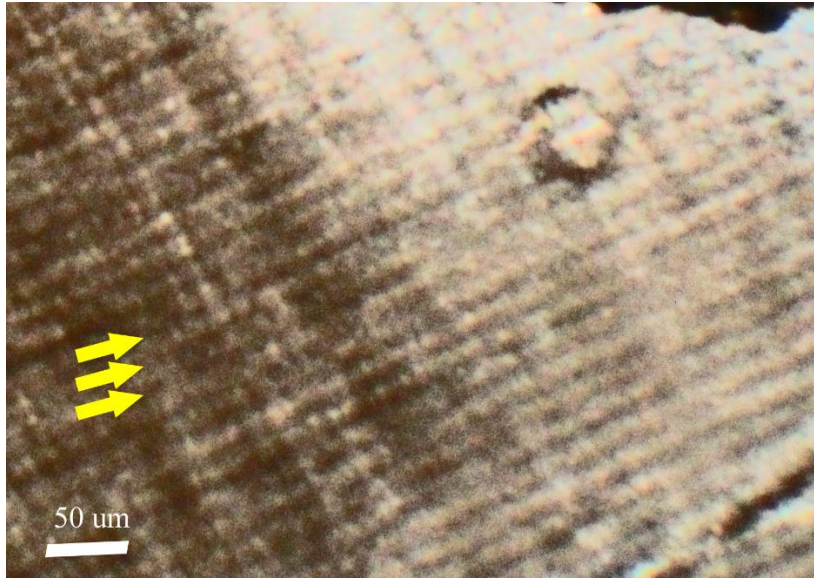
Figure 3.2. Dentine anomalies and increment-obscuring features observed in the Isle Royale moose population. A) A specimen with multiple tracts of sclerotic dentine marked with yellow arrowheads and a band of hypermineralized dentine marked with an asterisk (*). B) A specimen with a large, dark inner ring of hypermineralized dentine. C) A specimen with a band of granular dentine marked with a yellow arrow. D) A specimen stained and partially demineralized by a tree root that entered the mandibular canal. E-F) A specimen with granular-appearing dentin imaged under E) incident and F) transmitted light. The change in granule appearance indicates that they are air spaces.
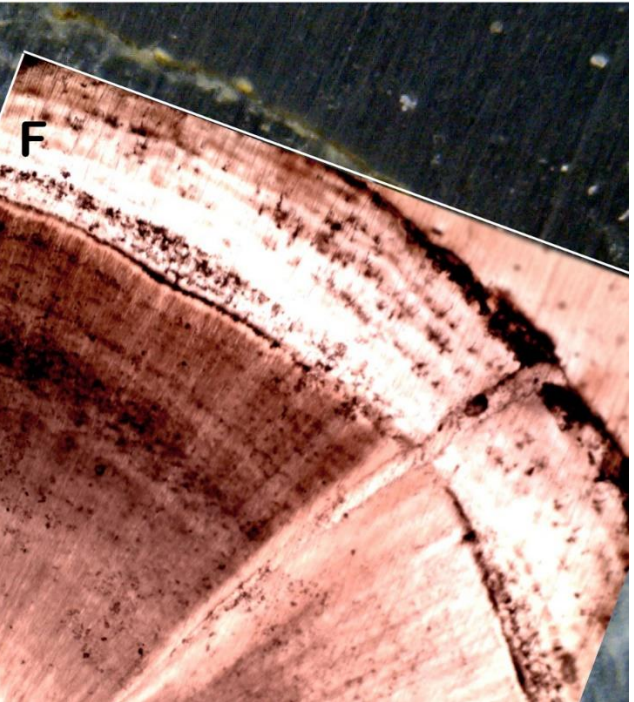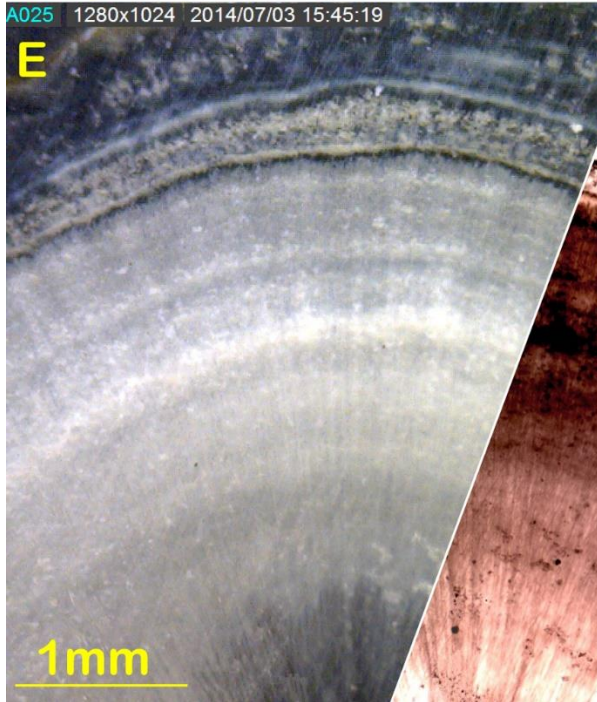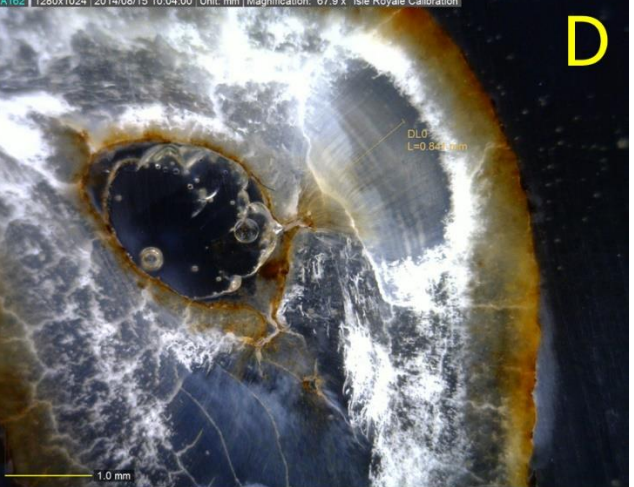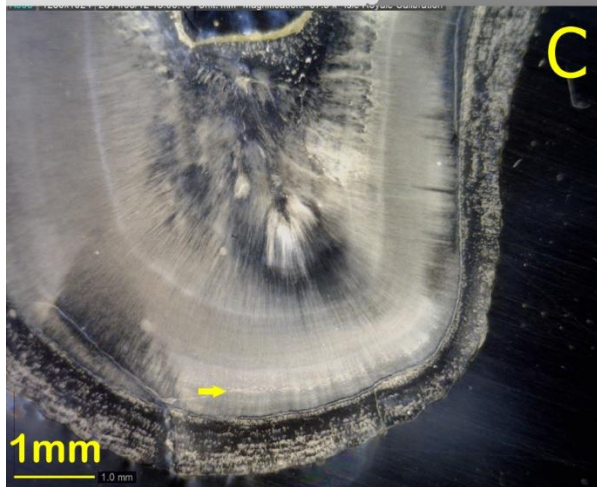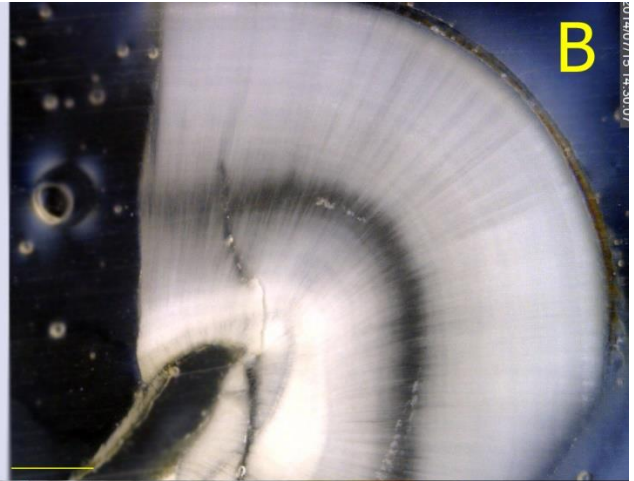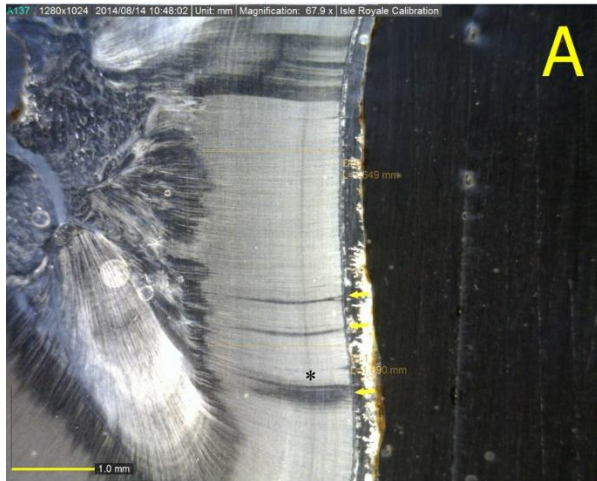
Figure 3.3. Diagram of a simplified tooth root labeled with dashed lines representing the three levels of sampling. The first transverse cut was made 4 mm apical to the cemento-enamel junction was *in situ*, Adapted from Bacchi, Ataís, et al. "Influence of post-thickness and material on the fracture strength of teeth with reduced coronal structure." *Journal of Conservative Dentistry* 16.2 (2013): 139.
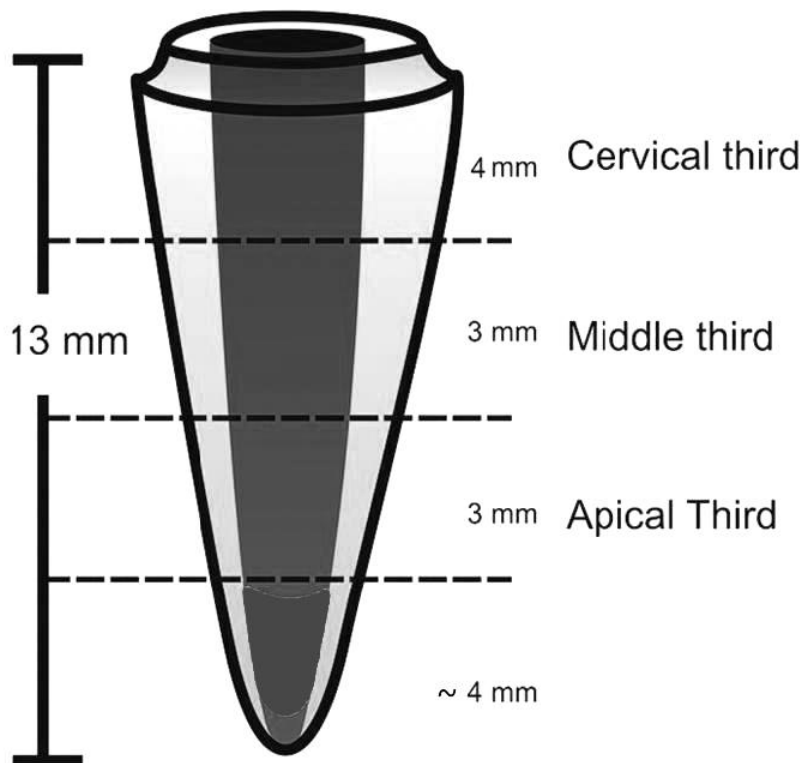
Figure 3.4. Diagram of stages in primary dentine formation in the root. Mineralization of older dentine occurs while new predentine is being secreted, thus both processes are occurring in all illustrations. Adapted from Sergeant, David E., and Douglas H. Pimlott. "Age determination in moose from sectioned incisor teeth." *The Journal of Wildlife Management* 23.3 (1959): 315-321.
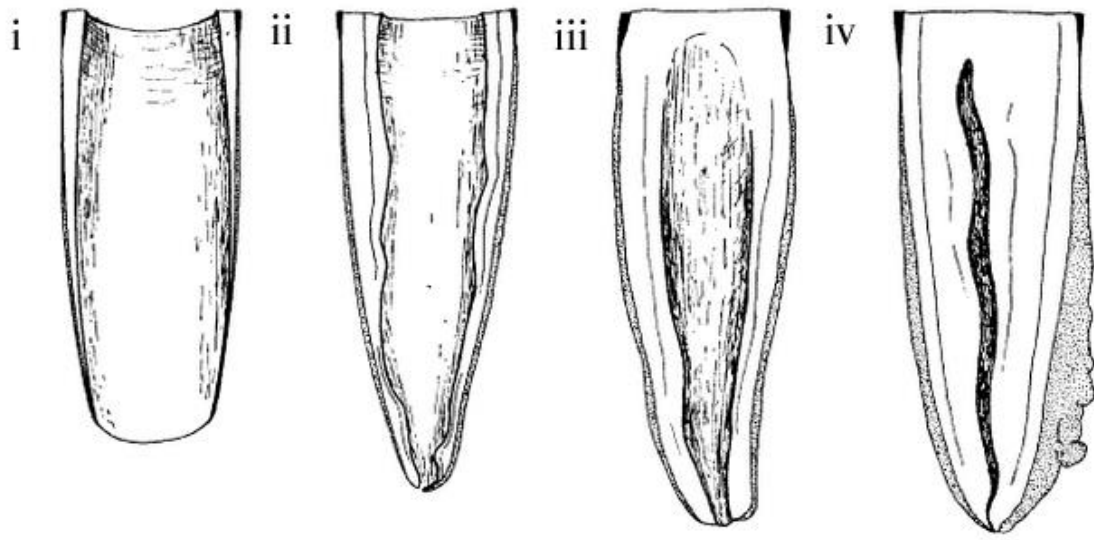
Figure 3.5. Histogram of observed increment widths in each tooth section and median value (black line). The overlap in values between each third of the root indicates there is not a significant seasonal reduction in growth rate during primary dentine growth.
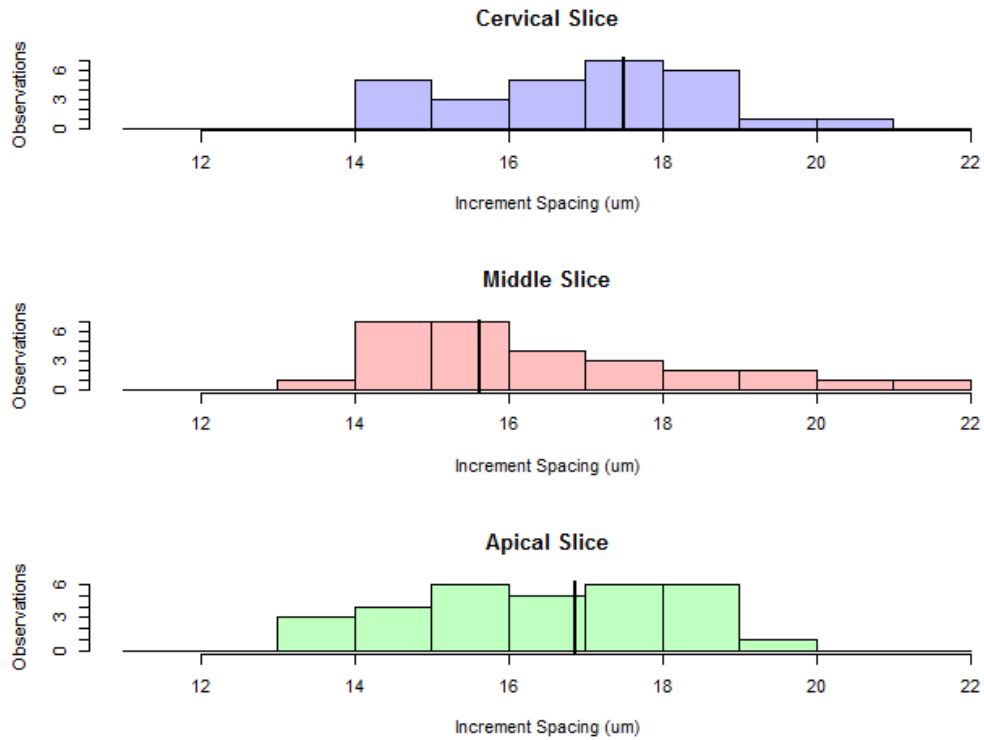
Figure 3.6. Average increment width relative to population density. Males and females are differentiated by symbol to illustrate the lack of sex differences in incremental growth of dentine. The population density threshold used to bin specimens into high vs. low density groups (Chapter. 2) is indicated with a red line.
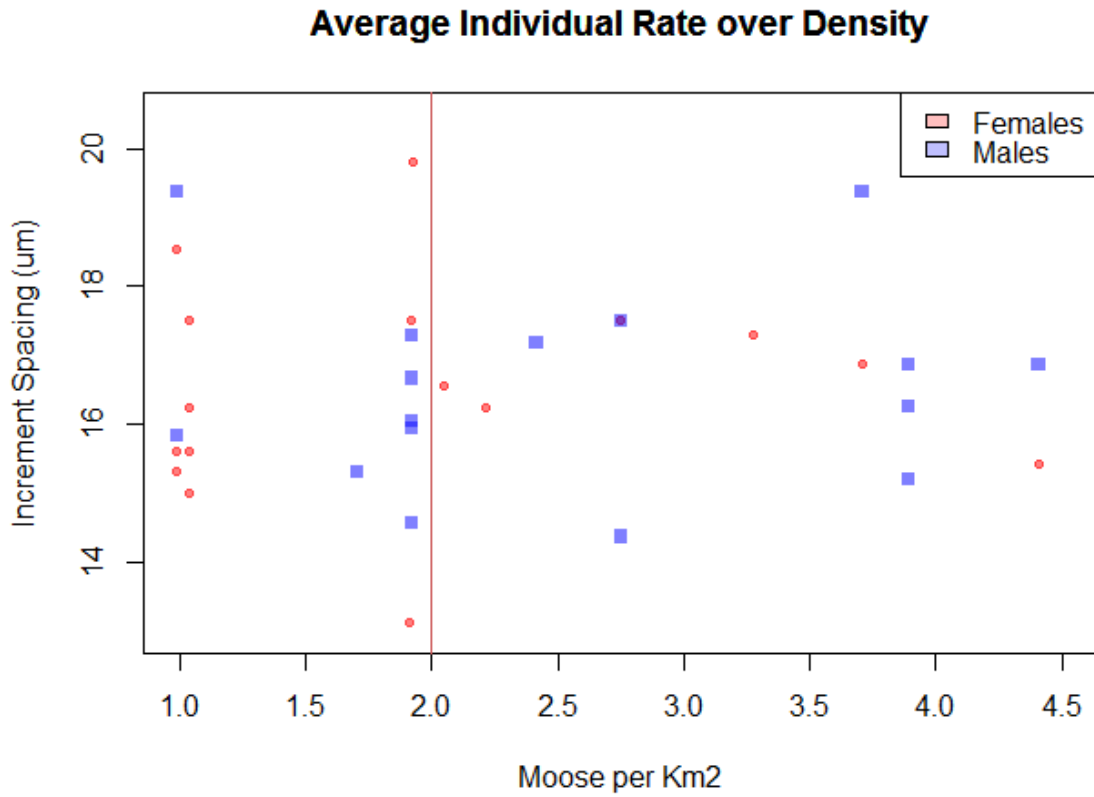
Figure 3.7. A) Population of IRNP moose by year with study periods labeled and shaded. Boxplot of B) averaged increment width C) cervical increment width. D) middle increment width E) apical increment width over study periods.
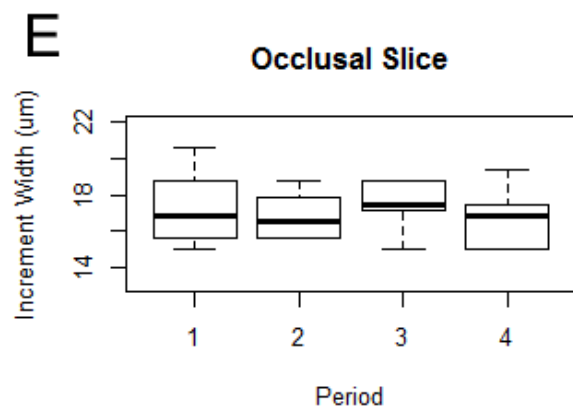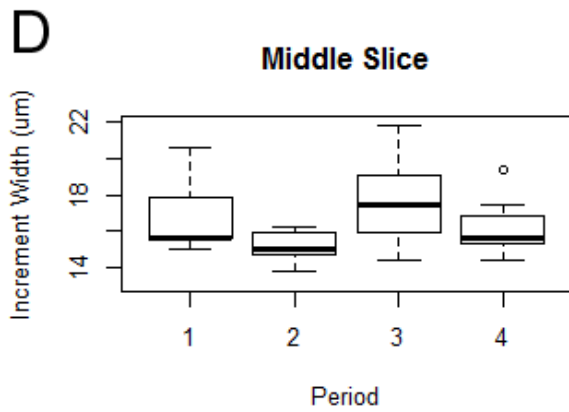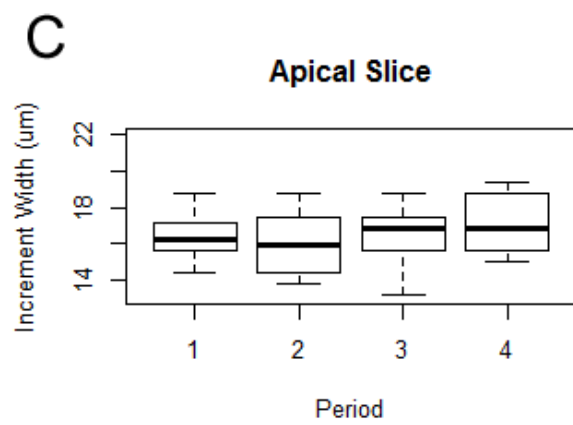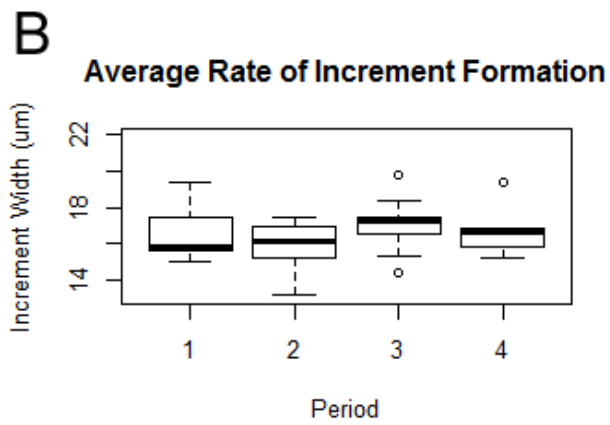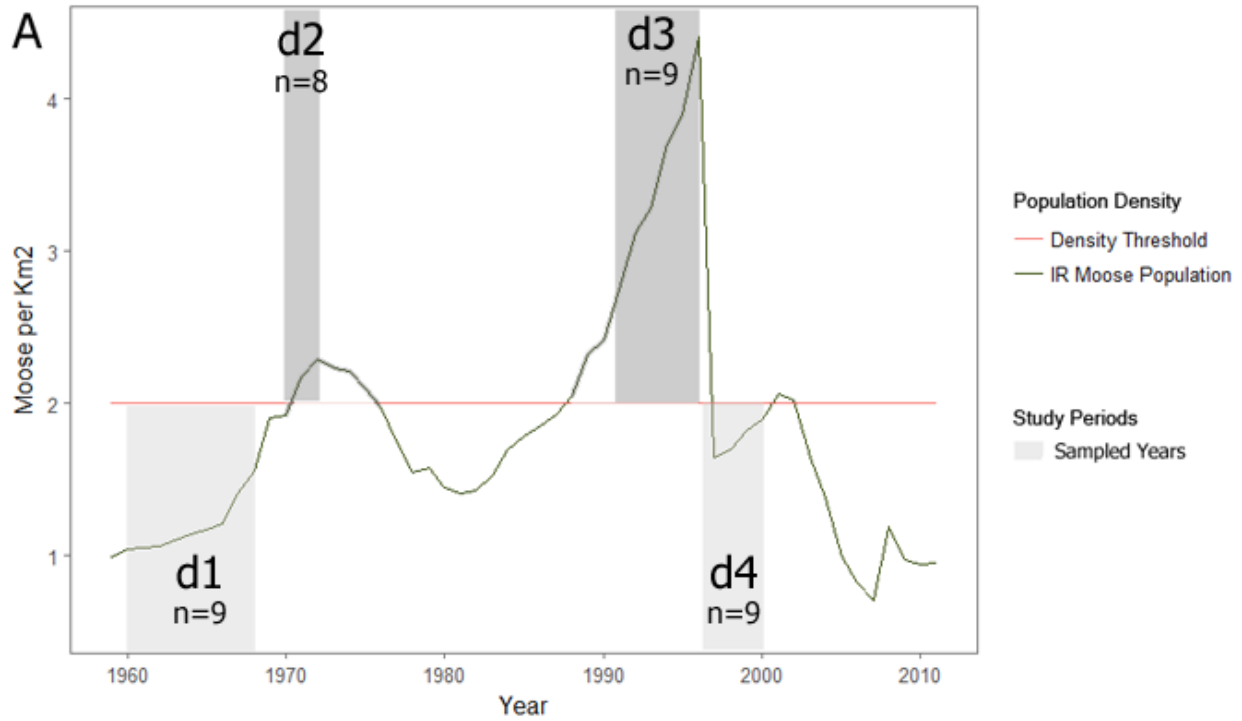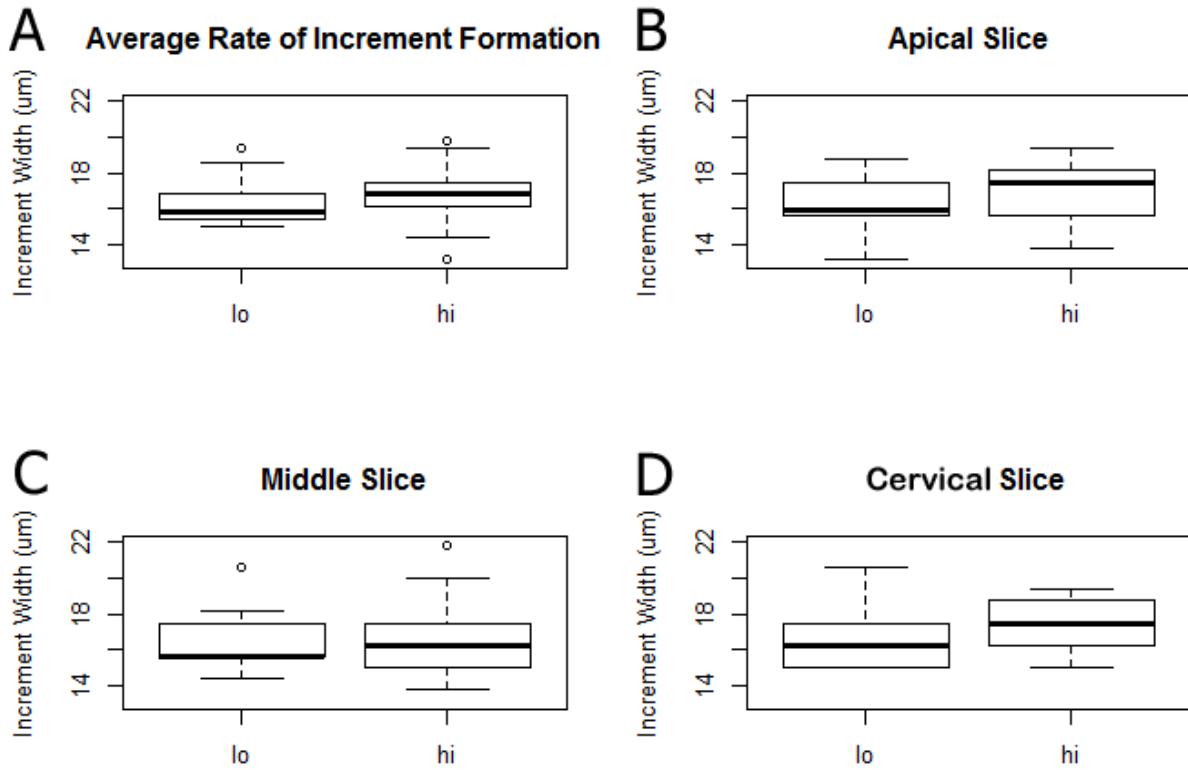
Figure 3.8. Boxplot of A) averaged increment width over study periods. B) cervical increment width. C) middle increment width D) apical increment width between moose born two years after high or low moose density.

REFERENCES

1.   Monlux WS. Hard Tissue Lesions Associated with Malnutrition. Iowa State Univerity Vet. 1961;24(2).

2.   Fisher DC. Season of death, growth rates, and life history of North American mammoths. In: West D, editor. Proceedings of the Internation Conference on Mammoth Site Studies Publication in Anthropology. University of Kansas; 2001. p. 122–35.

3.   Klevazel GA. Retrospective estimate of the individual history of life in population studies on mammals. Ontogenez. 2001;32(6):477–80.

4.   Fox DL. Growth increments in Gomphotherium tusks and implications for late Miocene climate change in North America. Palaeogeogr Palaeoclimatol Palaeoecol. 2000;156(3–4):327–48.

5.   Rinaldi C, Cole TM. Environmental seasonality and incremental growth rates of beaver (Castor canadensis) incisors: Implications for palaeobiology. In: Palaeogeography, Palaeoclimatology, Palaeoecology. 2004. p. 289–301.

6.   Dean MC, Scandrett AE. The relation between long-period incremental markings in dentine and daily cross-striations in enamel in human teeth. Arch Oral Biol. 1996;41(3):233–41.

7.   Carrick R, Csordas SE, Ingham SE. Studies on the southern elephant seal, Mirounga leonina (L.). IV. Breeding and development. Wildl Res. 1962;7(2):161–97.

8.   Miller SC, Omura TH, Smith LJ. Changes in dentin appositional rates during pregnancy and lactation in rats. J Dent Res. 1985;64(8):1062–4.

9.   Klevezal GA, Myrick ACJ. Marks in tooth dentine of female dolphins (Genus *Stenella*) as indicators of parturition. J Mammal. 1984;65(1):103–10.

10.   Manzanilla SR. The 1982-1983 El Niño event recorded in dentinal growth layers in teeth of Peruvian dusky dolphins (*Lagenorhynchusobscurus*). Can J Zool. 1988;67(July):2120–5.

11.   Klevezal GA, Mina M V. Daily layers and hibernation marks in incisor dentin of Sicista pseudonapaea and some biological remarks. Acta Theriol (Warsz). 1990;35(3–4):345–56.

12.   Rinaldi C. A record of hibernation in the incisor teeth of Recent and fossil marmots (Marmota flaviventris). In: Proc 11th Int Symp on Dental Morphology. 1999.

13.   Goodwin H, Michener G, Gonzalez D, Rinaldi C. Hibernation is recorded in lower incisors of recent and fossil ground squirrels (Spermophilus). J Mammal [Internet]. 2005;86(2):323. Available from: http://caslon.stanford.edu:3210/sfxlcl3?url_ver=Z39.88-

2004&ctx_ver=Z39.88-2004&ctx_enc=info:ofi/enc:UTF-8&rft_val_fmt=info:ofi/fmt:kev:mtx:journal&rft.genre=article&rft.issn=0022-2372&rft.coden=JOMAAL&rft.date=2005&rft.volume=86&rft.issue=2&rft.spage=323

14. Yilmaz S, Newman HN, Poole DFG. Diurnal periodicity of von Ebner growth lines in pig dentine. Arch Oral Biol. 1977;22(8–9):511–3.

15. Iinuma YM, Tanaka S, Kawasaki K, Kuwajima T, Nomura H, Suzuki M, et al. Dental incremental lines in Sika deer (Cervus nippon); polarized light and fluorescence microscopy of ground sections. J Vet Med Sci [Internet]. 2004;66(6):665–9. Available from: http://www.ncbi.nlm.nih.gov/pubmed/15240941

16. Pike-Tay A. Variability and synchrony of seasonal indicators in dental cementum microstructure of the Kaminiriak caribou population. Archeofauna Int J Archaeozoology. 1995;4:273–84.

17. Tonge H. Severe undernutrition in growing and adult animals. 1965;(14).

18. Silvia WJ, Peterson RO, Vucetich JA, Silvia WF, Silvia W. Variation in Metatarsal Morphology Among Subgroups of North American Moose (Alces alces). 1979;

19. Peterson RO, Vucetich JA, Beyer D, Schrage M. Phenotypic Variation in Moose : the Island Rule and the Moose of Isle Royale. 2011;47(Lieberman 2009):125–33.

20. Peterson RL. North American Moose. University of Toronto Press; 1950.

21. Manly RS, Hodge AHC. Density and Refractive Index Studies of Dental Hard Tissues I . Methods for Separation and Determination of Purity. :133–41.

22. Klevezal GA. Recording Structures of Mammals: determination of Age and Reconstruction of Life History. Mina M V, Oreshkin AV, editors. Rotterdam: A. A. Balkema; 1996.

23. Peterson RO. of Wolves on Isle Royale by. 1996;

24. Peterson R, McLaren B. Wolves , Moose , and Tree Rings on Isle Royale. Adv Sci. 2010;266(5190):1555–8.

25. Reshef DN, Reshef YA, Finucane HK, Grossman SR, Mcvean G, Turnbaugh PJ, et al. Detecting novel associations in large datasets. Science (80-). 2011;334(6062):1518–24.

26. Albanese D, Filosi M, Visintainer R, Riccadonna S, Jurman G, Furlanello C. minerva and minepy : a C engine for the MINE suite and its R , Python and MATLAB wrappers. 2013;29(3):407–8.

27. Hillson S. Teeth. Cambridge Manuals in Archaeology. 1986. 376 p.

28.	Vasiliadis L, Darling AI, Levers BGH. The amount and distribution of sclerotic human root dentine. Arch Oral Biol. 1983;28(7):645–9.

29.	Schour I, Hoffman AMM. Studies in Tooth Development I . 16 Microns Calcification Rhythm in the Enamel and Dentin from Fish to Man. J Dent Res. 1939;18(1):91–102.

30.	Dean MC, Cole TJ. Human Life History Evolution Explains Dissociation between the Timing of Tooth Eruption and Peak Rates of Root Growth. 2013;8(1).

31.	Liber O, Wahlstrom K. Habitat stability and litter size in the Cervidae; a comparative analysis. University of Stockholm, Sweden; 1995.

32.	Gaillard J-M. Are moose only a large deer?: Some life history considerations. Alces. 2007;43:1–11.

33.	DeIguidice GD, Peterson RO, Samuel WM. Trends of Winter Nutritional Restriction , Ticks , and Numbers of Moose on Isle Royale. Published by : Wiley on behalf of the Wildlife Society Stable URL : http://www.jstor.org/s. 2017;61(3):895–903.

34.	Mangel M, Munch SB. A Life-History Perspective on Short- and Long-Term Consequences of Compensatory Growth. Am Nat [Internet]. 2005;166(6):E155–76. Available from: http://www.journals.uchicago.edu/doi/10.1086/444439

35.	Hector KL, Nakagawa S. Quantitative analysis of compensatory and catch-up growth in diverse taxa. J Anim Ecol. 2012;81(3):583–93.

36.	Dale BW, Adams LG, Collins WB, Joly K, Valkenburg P, Tobey R. Stochastic and Compensatory Effects Limit Persistence of Variation in Body Mass of Young Caribou. J Mammal. 2008;89(5):1130–5.

37.	Watkins W. Compensatory growth of wapiti (Cervus elaphus) on aspen parkland ranges. Can J … [Internet]. 1991;69:1682–8. Available from: http://www.nrcresearchpress.com/doi/abs/10.1139/z91-233

38.	Luke DA, Tonge CH, Reid DJ. Effects of rehabilitation on the jaws and teeth of protein-deficient and calorie-deficient pigs. Cells Tissues Organs. 1981;110(4):299–305.

39.	Festa-bianchet M, Jorgenson JT, Réale D, Re D, Réale D, Re D. Early development, adult mass, and reproductive success in bighorn sheep. Behav Ecol [Internet]. 2000;11(6):633–9. Available from: http://www.scopus.com/inward/record.url?eid=2-s2.0-0034580832&partnerID=40&md5=dba15274fd0cc386ada6044900993ded

40.	Wairimu S, Hudson RJ. Foraging dynamics of wapiti stags (Cervus elaphus) during compensatory growth. Appl Anim Behav Sci. 1993;36(1):65–79.

41.	Suttie JM, Goodall ED, Pennie K, Kay RN. Winter food restriction and summer

compensation in red deer stags (Cervus elaphus). Br J Nutr. 1983;50:737–47.

42.   White RG. Nutritional in relation to season, lactation, and growth of north temperate deer. In: The biology of deer. Springer New York; 1992. p. 404–17.

43.   Keech MA, Boertje RD, Bowyer RT, Dale BW. Effects of birth weight on growth of young moose: do low-weight neonates compensate? Vol. 35, Alces. 1999. p. 51–7.

44.   Solberg E, Garel M, Heim M, Grøtan V, Sæther B-E. Lack of compensatory body growth in a high performance moose Alces alces population. Oecologia [Internet]. 2008;158(3):485–98. Available from: http://dx.doi.org/10.1007/s00442-008-1158-z

45.   Ten-Cate AR. Oral Histology: Development, Structure and Function. 3rd ed. The C.V. Mosby Company; 1989. 159-161 p.

46.   Klevezal GA, Phillips CJ. The nature of sclerotic dentine in the teeth of mammals: new clues to life history. In: 66th Annual Meeting of American Society of Mammologists. 1986. p. 15–9.